

# Variational Robust Kalman Filters: A Unified Framework

Shilei Li, Dawei Shi, Hao Yu, Ling Shi

## Abstract

Robustness and adaptivity are two competing objectives in Kalman filters (KF). Robustness involves temporarily inflating prior estimates of noise covariances, while adaptivity updates prior beliefs using real-time information. In practical applications, both process and measurement noise can be influenced by outliers, be time-varying, or both. Existing works may not effectively address the above complex noise scenarios, as there is an intrinsic incompatibility between robust filters and adaptive filters. In this work, we propose a unified variational robust Kalman filter, built on a Student's  $t$ -distribution induced loss function and variational inference, and solved through fixed-point iteration in a computationally efficient manner. We demonstrate that robustness can be understood as a prerequisite for adaptivity, making it possible to merge the above two competing goals into a single framework through switching rules. Additionally, our proposed filter can recover conventional KF, robust KF, and adaptive KF by adjusting parameters, and can suppress both the imperfect process and measurement noise, enabling it to perform superiorly in complex noise environments. Simulations verify the effectiveness of the proposed method.

## Index Terms

Student's  $t$ -distribution, robustness and adaptability, fixed-point iteration, variational inference

## I. Introduction

State estimation aims to infer the latent states of a system from a mathematical model and noisy measurements, serving as a critical foundation for numerous fields, including robotics [1], finance [2], medical imaging [3], and meteorology [4]. The Kalman filter, co-developed by Kalman and Bucy, is a cornerstone in state estimation, providing optimal estimates in the mean squared error sense. Despite its theoretical elegance, the Kalman filter's reliance on Gaussian noise assumptions limits its efficacy in complex systems subject to imprecise noise covariance [5] or unknown noise models [6].

Research on filtering with non-Gaussian noise or unknown covariance is active. There are two main lines of research efforts: robustness and adaptability. The vulnerability of the Kalman filter to outliers has been found in its early history [7]. To enhance its robustness,  $H_\infty$  filter, sometimes called minimax filter, is derived under the game theory framework [8]. To combat gross errors, some M-estimation-based estimators were coined, e.g., Huber-based filter [9],  $\ell_1$  norm-based Kalman filter [10]. An alternative approach of deriving robust estimators is to exploit the heavy-tailed distributions, including the Laplace-based filter [11] and Student's  $t$ -based filter [12]. Recently, the correntropy and statistical similarity measure, given their roots in the information-theoretic learning [13] and statistical learning [14], were utilized for algorithm derivation and achieving satisfactory results, including maximum correntropy Kalman filter (MCKF) [15]–[17] and SSM-based Kalman filter (SSMKF) [18]. Both MCKF and SSMKF utilized a fixed-point iteration in optimization, which exhibited a higher computation efficiency than the gradient descent-based algorithms [19], [20]. Unfortunately, although the convergence of the fixed-point algorithm has been proved for a specific robust loss [17], [21], a more comprehensive applicable scope (i.e., which type of robust losses can be solved by fixed-point iteration) of this method is still missing. In this work, we mitigate this gap and provide sufficient conditions (Theorem 3) for identifying which robust losses can be addressed using this method and provide some examples.

Another prominent line is adaptive filtering, which can be broadly categorized into Bayesian, maximum likelihood [22], covariance matching [23], and variational Bayesian (VB) methods. Among these, Bayesian approaches are the most general, exemplified by techniques such as the interacting multiple model Kalman filter and partial filters. However, methods involving multiple models and sampling-based estimators often suffer from high computational complexity. In contrast, VB methods provide a more computationally efficient alternative by approximating posterior inference through conjugate distributions. A pioneering work in this area was presented by Simo [24], focusing on adaptive measurement covariance. This was later extended to include adaptive process and measurement covariance [25], along with nonlinear counterparts such as the unscented and cubature Kalman filters [26], [27]. Although many variants of variational Bayesian Kalman filter (VBKF) had been developed, one of its key problem, the covariance tracking speed

Shilei Li, Dawei Shi, and Hao Yu are with School of Automation, Beijing Institute of Technology, Beijing 100081, China (e-mail: shileili@bit.edu.cn, yuhao@bit.edu.cn, dawei@bit.edu.cn).

Ling Shi is with the Department of Electronic and Computer Engineering, The Hong Kong University of Science and Technology, Kowloon, Hong Kong (e-mail: eesling@ust.hk).

and the corresponding tracking cost, are not fully exploited. In this work, we provide the corresponding covariance tracking speed (Theorems 5 and 6), and reveal an inherent trade-off between convergence speed and steady state variance regarding the forgetting factor.

Many previous works concentrate on either robustness [6], [28], [29] or adaptability [24], [30]. It is worth clarifying that the terminology “robust adaptive” mentioned in [29] actually referred to adaptive robustness and hence falls into the first class (robustness). The VBKF [24], [30], although adjusting both shape and scale hyper-parameters, falls into the second class (adaptivity). To the best of the authors’ knowledge, only a limited number of studies consider the coexistence of time-varying covariance and outliers [31], [32], whereas their solutions were a combination of VB and robust loss techniques, resulting in complex and computationally demanding solutions. For instance, Chang [31] proposed an innovation-based measure to switch between the standard Kalman filter, the fading memory Kalman filter, and the robust Kalman filter to balance between robustness and adaptability. Li et al. [32] addressed this problem by designing a variational Huber-based filter by combining M-estimation with VB approximation. In this work, we prove that the robust filter (under the student’s  $t$ -induced loss) can be understood as a prerequisite of adaptive filters (VBKF), allowing to solve the robust adaptive problem sequentially (Theorem 4). Some switching rules are subsequently designed to enhance the filter’s ability in complex noise scenarios. Our developed filters can recover KF, robust KF, VBKF, and can encode our prior belief on noise characteristics (contaminated by outliers, being adaptive, or both) into a unified framework easily. The contributions of this paper are summarized as follows.

- A sufficient condition for the convergence of fixed-point iteration under a class of robust losses is provided in Theorem 3. Additionally, several robust filters, including the Student’s  $t$ -based Kalman filter (STKF, Algorithm 1), are derived using a fixed-point iteration solution.
- It is revealed that the STKF is identical to the VBKF [24] with fixed prior distributions in Theorem 4, thereby establishing a connection between robust and adaptive filters. Meanwhile, Theorems 5 and 6 demonstrated that there is a trade-off between covariance convergence speed and steady-state variance regarding the selection of forgetting factor  $\rho$ .
- Instead of solving a set of coupled equations in variational-based filters, this work solves the same problem sequentially and identically: robust estimation and hyperparameter update (see Algorithm 2). The proposed filter can recover the KF, robust KF, and adaptive KF easily by tuning the hyperparameters, providing a unified framework for versatile applications.

The remainder of this paper is organized as follows. Section II introduces some preliminaries. Section III derives a family of robust filters with guaranteed convergence. Section IV develops some robust adaptive filters. Section V provides some simulations. Section VI concludes the paper.

**Notations:** The transpose of a matrix  $A$  is denoted by  $A^T$ .  $X \succ 0$  ( $X \geq 0$ ) denotes  $X$  is positive definite (semi-positive definite) matrix. The Gaussian distribution with mean  $\mu$  and covariance  $\Sigma$  is denoted by  $\mathcal{N}(\mu, \Sigma)$ . The expectation of a random variable  $X$  or random vector  $\mathcal{X}$  is denoted by  $E(X)$  or  $E(\mathcal{X})$ .

## II. Preliminaries

We begin by presenting the necessary preliminaries and lemmas, followed by the problem statement.

### A. The Student’s $t$ -distribution

The probability distribution functions (PDF) of Student’s  $t$ -distribution, Gaussian distribution, and inverse Gamma distribution of random variable  $X$  are given as follows:

$$\text{St}(x | \nu, \mu, \tau^2) = \frac{\Gamma(\frac{\nu+1}{2})}{\Gamma(\frac{\nu}{2}) \sqrt{\pi \nu \tau^2}} \left(1 + \frac{1}{\nu} \frac{(x - \mu)^2}{\tau^2}\right)^{-(\nu+1)/2}, \quad (1a)$$

$$\mathcal{N}(x | \mu, \tau^2) = \frac{1}{\sqrt{2\pi}\sigma} \exp\left(-\frac{1}{2} \frac{(x - \mu)^2}{\tau^2}\right), \quad (1b)$$

$$\text{Inv-Gam}(x | a, b) = \frac{b^a}{\Gamma(a)} (1/x)^{a+1} \exp(-b/x), \quad (1c)$$

where  $\text{St}(x | \nu, \mu, \tau^2)$  denotes the Student’s  $t$ -distribution with degrees of freedom (DOF)  $\nu$ , mean  $\mu$ , and scale parameter  $\tau^2$ ,  $\mathcal{N}(x | \mu, \tau^2)$  denotes the Gaussian distribution with mean  $\mu$  and covariance  $\tau^2$ , and  $\text{Inv-Gam}(x | a, b)$  denotes the inverse-Gamma distribution with shape parameter  $a$  and scale parameter  $b$  [33].

**Lemma 1** ([33]): The Student’s  $t$  distribution  $\text{St}(x | \nu, \mu, \tau^2)$  is a compounding distribution composed of a Gaussian distribution and Inverse-Gamma distribution, i.e., it is equivalent to

$$x \sim \mathcal{N}(\mu, \lambda), \quad (2)$$

where  $\lambda$  follows

$$\lambda \sim \text{Inv-Gam}(\lambda | \frac{\nu}{2}, \frac{\nu \tau^2}{2}). \quad (3)$$

According to the robustness definition in [34], the Student's  $t$ -distribution is outlier prone of order 1, and it can reject up to  $m$  outliers if there are at least  $2m$  observations [35]. Taking the logarithm on the right side of (1a) and ignoring the constant terms, we obtain the Student's  $t$ -induced loss  $\mathcal{L}_{st}^*$  as follows

$$\mathcal{L}_{st}^* = \frac{\nu + 1}{2} \log \left( 1 + \frac{e^2}{\nu \tau^2} \right). \quad (4)$$

Before proceeding, we provide the following lemma and properties.

**Lemma 2 (Invariant Loss):** Let the error vector  $e = [e_1, e_2, \dots, e_l]^T \in \mathbb{R}^l$  consists of statistically independent components (i.e.,  $p(e_i e_j) = p(e_i)p(e_j)$  with  $i \neq j$ ). Then, the following two losses give the identical results:

$$\mathcal{L}_{st}^* = \sum_{i=1}^l \frac{\nu_i + c}{2} \log \left( 1 + \frac{e_i^2}{\nu_i \tau_i^2} \right), \quad (5a)$$

$$\mathcal{L}_{st} = \sum_{i=1}^l \frac{\nu_i}{2} \log \left( 1 + \frac{e_i^2}{\nu_i \tau_i^2} \right), \quad (5b)$$

where  $\nu_i$  and  $\tau_i^2$  are constants and  $c \in \mathbb{R}$  is a scalar.

The proof of the lemma is in Appendix VI-A. By analogy with the obtainment of  $\mathcal{L}_{st}^*$ , we obtain the Gaussian-induced loss  $\mathcal{L}_{gau}$  according to (1b). We compare  $\mathcal{L}_{st}$  and  $\mathcal{L}_{gau}$  as follows

$$\mathcal{L}_{st} = \frac{\nu}{2} \log \left( 1 + \frac{e^2}{\nu \tau^2} \right), \quad \mathcal{L}_{gau} = \frac{1}{2} \frac{e^2}{\tau^2}. \quad (6)$$

Its influence functions, measuring the derivative of the loss with respect to the error, are given as

$$\frac{\partial \mathcal{L}_{st}}{\partial e} = \frac{\nu e}{\nu \tau^2 + e^2}, \quad \frac{\partial \mathcal{L}_{gau}}{\partial e} = \frac{e}{\tau^2}. \quad (7)$$

**Property 1:** As  $\nu \rightarrow \infty$ , one has  $\mathcal{L}_{st} = \mathcal{L}_{gau}$ . As  $\nu = 1$ ,  $\mathcal{L}_{st}$  becomes Cauchy loss corresponding to Cauchy distribution.

**Proof 1:** According to  $\lim_{x \rightarrow 0} \log(1 + x) = x$ , it follows that

$$\lim_{\nu \rightarrow \infty} \frac{\nu}{2} \log \left( 1 + \frac{e^2}{\nu \tau^2} \right) = \frac{1}{2} \frac{e^2}{\tau^2} \quad (8)$$

and hence  $\mathcal{L}_{st} = \mathcal{L}_{gau}$  as  $\nu \rightarrow \infty$ . As  $\nu = 1$ , one observes that  $\mathcal{L}_{st} = \frac{1}{2} \log \left( 1 + \frac{e^2}{\tau^2} \right)$  which becomes Cauchy loss and corresponds to Cauchy distribution. This completes the proof.

**Property 2:** The loss  $\mathcal{L}_{st}$  is convex with the region  $[-\sqrt{\nu}\tau, \sqrt{\nu}\tau]$ , and is concave in other regions.

**Proof 2:** It is easy to obtain the Hessian matrix of  $\mathcal{L}_{st}$  as follows

$$H(\mathcal{L}_{st}) = \frac{\partial^2 \mathcal{L}_{st}}{\partial e^2} = \frac{\nu(\nu\tau^2 - e^2)}{(\nu\tau^2 + e^2)^2}. \quad (9)$$

It is obvious that  $H(\mathcal{L}_{st}) \geq 0$  as  $e \in [-\sqrt{\nu}\tau, \sqrt{\nu}\tau]$  and  $H(\mathcal{L}_{st}) < 0$  otherwise. This completes the proof.

**Property 3:** As  $\nu \rightarrow \infty$ , the PDF of latent variable  $\lambda$  (see (3)) becomes a shifted Dirac delta function  $\delta(\lambda - \tau^2)$ .

**Proof 3:** According to (3), one has

$$p(\lambda) = \frac{(\nu\tau^2/2)^{\nu/2}}{\Gamma(\nu/2)} (1/\lambda)^{\nu/2+1} \exp\left(-\frac{\nu\tau^2}{2\lambda}\right).$$

By applying Stirling's approximation, one has  $\Gamma(\nu/2) \sim \sqrt{2\pi}(\frac{\nu}{2})^{\nu/2-1} \exp(-\nu/2)$  as  $\nu \rightarrow \infty$ , it follows that

$$\begin{aligned} \lim_{\nu \rightarrow \infty} p(\lambda) &= \frac{(\nu\tau^2/2)^{\nu/2}}{\sqrt{2\pi}(\frac{\nu}{2})^{\nu/2-1}} (1/\lambda)^{\nu/2+1} \exp\left(-\frac{\lambda\nu - \nu\tau^2}{2\lambda}\right) \\ &= \frac{\nu}{2\sqrt{2\pi}\lambda} \left(\frac{\tau^2}{\lambda}\right)^{\nu/2} \exp\left(-\frac{\lambda\nu - \nu\tau^2}{2\lambda}\right). \end{aligned} \quad (10)$$

One observes that  $\lim_{\nu \rightarrow \infty} p(\lambda) \rightarrow \infty$  as  $\lambda = \tau^2$  and tend to 0 for any other  $\lambda \neq 0$ . This completes the proof.

**Remark 1:** The degrees of freedom,  $\nu$ , determines the confidence level of the unknown variance  $\tau^2$  in  $\mathcal{L}_{st}$ . A smaller  $\nu$  indicates a higher degree of uncertainty about the variance  $\tau^2$ , and vice versa.

The loss and influence functions of  $\mathcal{L}_{st}$  and  $\mathcal{L}_{gau}$ , as well as their corresponding PDFs and the induced latent variable's PDF in  $\mathcal{L}_{st}$  are visualized in Fig. 1. One observes that the influence function of  $\mathcal{L}_{st}$  has a redescending property,

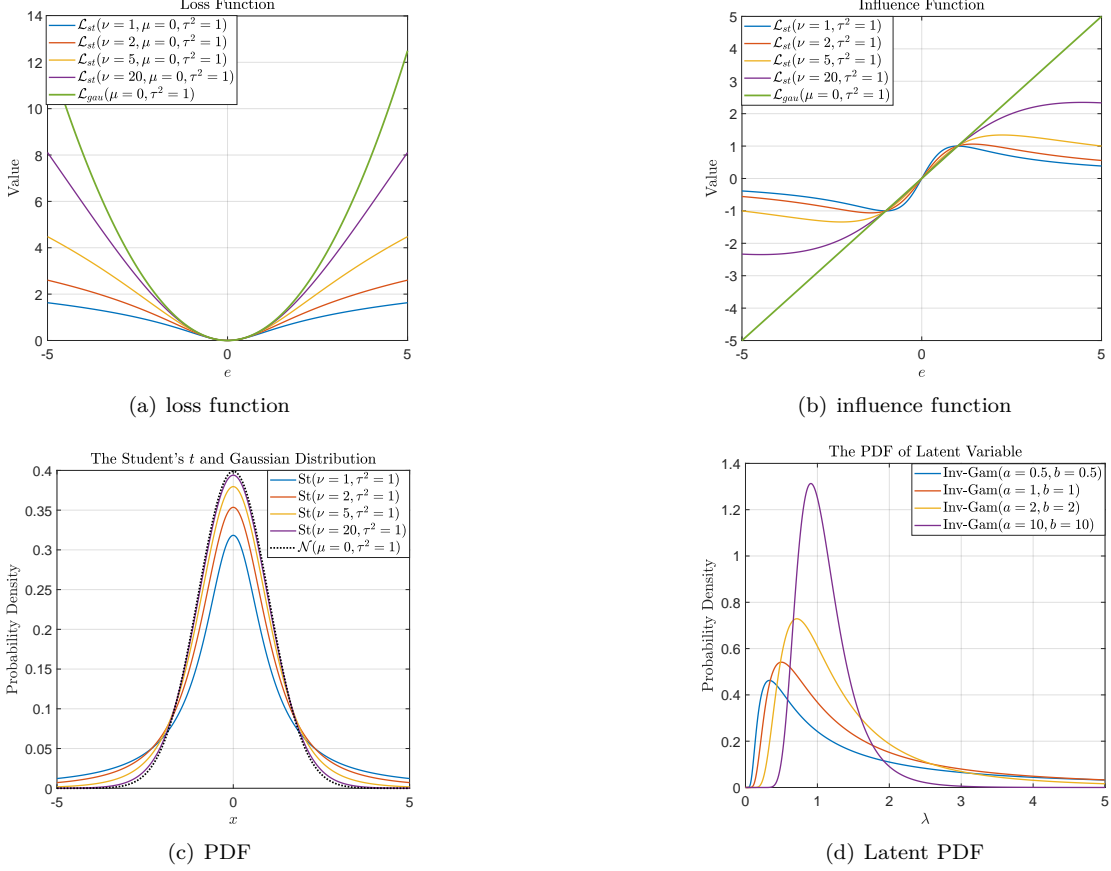


Fig. 1. The visualization of  $\mathcal{L}_{st}$  and  $\mathcal{L}_{gau}$  as well as their influence functions and induced PDFs. (a) The loss function of  $\mathcal{L}_{st}$  and  $\mathcal{L}_{gau}$ . (b) The influence function of  $\mathcal{L}_{st}$  and  $\mathcal{L}_{gau}$ . (c) The mapped Student's t distribution and Gaussian distribution. (d) The PDF of latent variable  $\lambda$ .

indicating its robustness to absolute errors that are much greater than  $\sqrt{\nu}\tau$ . According to Properties 1, 2, and 3, we have the following insights:

- The parameter  $\tau^2$  describes the variance of the latent Gaussian distribution.
- The parameter  $\nu$  reflects how confident we are about the latent variance  $\tau^2$ .

The above insights highlight the importance of  $\nu$  and  $\tau^2$  when using  $\mathcal{L}_{st}$  as a cost function.

## B. Problem Statement

We consider the following linear system:

$$\begin{aligned} x_{k+1} &= Ax_k + w_k \\ y_k &= Cx_k + v_k \end{aligned} \tag{11}$$

where  $A \in \mathbb{R}^{n \times n}$  and  $C \in \mathbb{R}^{m \times n}$  are state transfer and observation matrices. The process noise  $w_k$  and measurement noise  $v_k$  are uncorrelated zero-mean random noises with positive-definite covariances  $Q_k$  and  $R_k$ . The initial state  $x_0$  is zero-mean Gaussian with known covariance matrix  $P_0$ , and is independent of  $w_k$  and  $v_k$  for all  $k > 0$ . Distinct from the constant  $Q_k$  and  $R_k$  in standard KF, we consider that the noise covariance may be time-varying and occasionally contaminated by outliers, i.e.,

$$\begin{aligned} w_k &\sim \epsilon_w \mathcal{N}(0, Q_k) + (1 - \epsilon_w) p_{ol}(o_w), \\ v_k &\sim \epsilon_v \mathcal{N}(0, R_k) + (1 - \epsilon_v) p_{ol}(o_v), \end{aligned} \tag{12}$$

where  $Q_k > 0$  and  $R_k > 0$  are time-varying positive definite matrices,  $0 < \epsilon_w \leq 1$  and  $0 < \epsilon_v \leq 1$  are coefficients, and  $p_{ol}(o_w)$  and  $p_{ol}(o_v)$  are unknown outlier distributions. Note that (12) reduces to the standard KF by setting  $Q_k \triangleq Q$ ,  $R_k \triangleq R$ , and  $\epsilon_w = \epsilon_v = 1$ . It simplifies to the robust filtering problem by using  $Q_k \triangleq Q$ ,  $R_k \triangleq R$  with  $0 < \epsilon_w < 1$  and  $0 < \epsilon_v < 1$ , and becomes the adaptive filtering problem by using  $\epsilon_w = \epsilon_v = 1$ . This work provides a unified framework for both robust and adaptive estimators. A visualization of some types of noise considered in this work is given in Fig. 2.

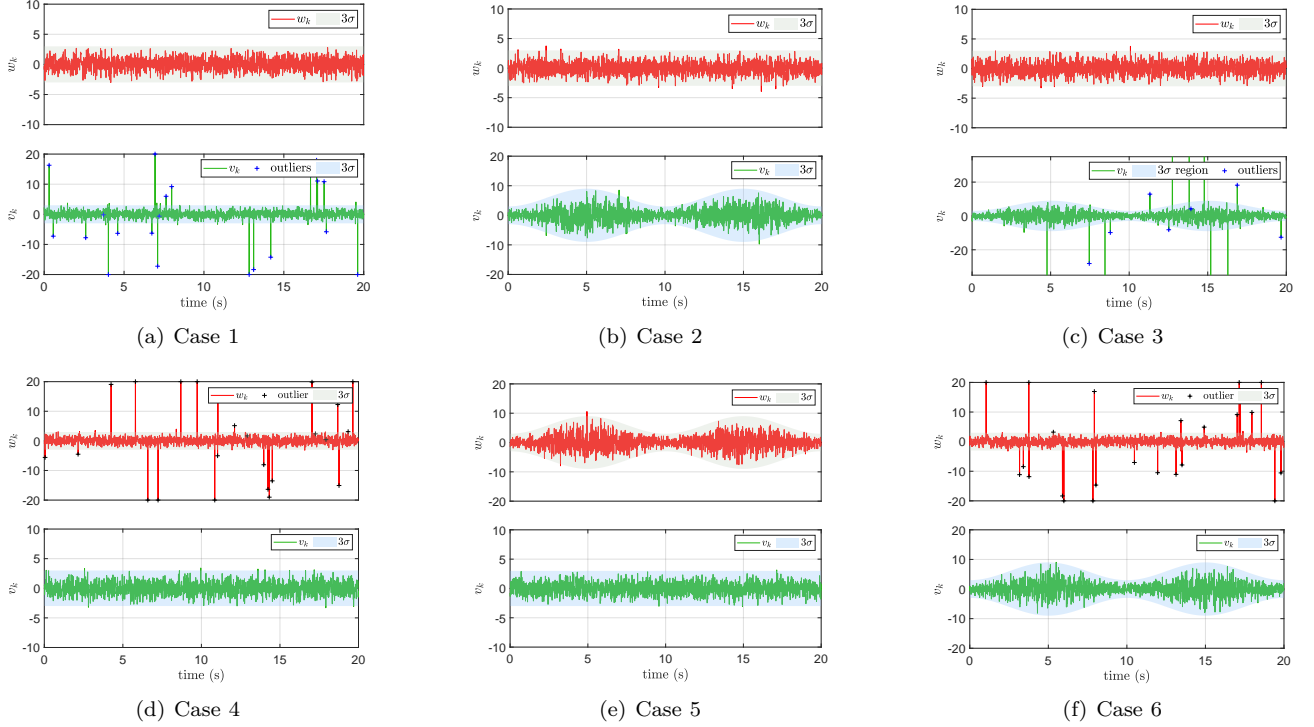


Fig. 2. Some noise scenarios considered in this work (but not limited to these examples). The first, second, and third column corresponds to Scenario 1, 2, and 3. The data with an absolute value bigger than 20 are visualized as  $\pm 20$ . (a) Case 1:  $w_k \sim \mathcal{N}(0, 1)$ ,  $v_k \sim 0.99\mathcal{N}(0, 1) + 0.01\mathcal{N}(0, 400)$ . (b) Case 2:  $w_k \sim \mathcal{N}(0, 1)$ ,  $v_k \sim \mathcal{N}(0, R_{k,t})$  where  $R_{k,t} = (1 + 2|\sin(0.1\pi t)|)^2$ . (c) Case 3:  $w_k \sim \mathcal{N}(0, 1)$ ,  $v_k \sim 0.99\mathcal{N}(0, R_{k,t}) + 0.01\mathcal{N}(0, 400)$ . (d) Case 4:  $w_k \sim 0.99\mathcal{N}(0, 1) + 0.01\mathcal{N}(0, 400)$ ,  $v_k \sim \mathcal{N}(0, 1)$ . (e) Case 5:  $w_k \sim 0.99\mathcal{N}(0, R_{k,t}) + 0.01\mathcal{N}(0, 400)$ ,  $v_k \sim \mathcal{N}(0, 1)$ . (f) Case 6:  $w_k \sim 0.99\mathcal{N}(0, 1) + 0.01\mathcal{N}(0, 400)$ ,  $v_k \sim N(0, R_{k,t})$ .

### III. Main Results

In this section, we first present a robust filter under  $\mathcal{L}_{st}$  with fixed hyperparameters. Next, we establish a connection between the robust filter and the adaptive filter. Finally, we update the hyperparameters using variational inference and design a switching rule for scenarios where outliers and time-varying noise coexist.

#### A. A Class of Robust Filters

By assigning the measurement noise  $v_k$  a nominal covariance, i.e.,  $v_k \sim \mathcal{N}(0, R_k^*)$  and denoting  $t_k = B_k^{-1}(x_k^-)$ ,  $W_k = B_k^{-1}(C)$ ,  $\zeta_k = B_k^{-1}(w_k)$ , and  $B_k B_k^T = \begin{bmatrix} P_k^- & 0 \\ 0 & R_k^* \end{bmatrix}$  ( $x_k^-$  and  $P_k^-$  denote the prior estimate of state and error covariance), one can rewrite (11) as

$$t_k = W_k x_k + \zeta_k, \quad (13)$$

where  $\zeta_k$  is the normalized measurement noise with identity covariance when  $w_k$  and  $v_k$  are Gaussian, i.e.,  $E(\zeta_k^T \zeta_k) = I$ . Instead of minimizing the least squares loss  $\|e_k\|_2^2$  where  $e_k = t_k - W_k x_k \in \mathbb{R}^{n+m}$  as done in KF [6], we minimize the following Student's  $t$ -based loss

$$J = \sum_{i=1}^l \frac{\nu_i}{2} \log(1 + (e_{i,k}^T e_{i,k}) / (\nu_i \cdot \tau_i^2)), \quad (14)$$

where  $l = n + m$  and  $e_{i,k} = t_{i,k} - w_{i,k} x_k$  which denotes  $i$ -th element of  $e_k$ . By letting  $\frac{\partial J}{\partial x_k} = 0$ , one has

$$x_k = \left( \sum_{i=1}^l \frac{\nu_i w_i^T w_i}{\nu_i \tau_i^2 + e_{i,k}^T e_{i,k}} \right)^{-1} \left( \sum_{i=1}^l \frac{\nu_i w_i^T t_i}{\nu_i \tau_i^2 + e_{i,k}^T e_{i,k}} \right). \quad (15)$$

It can be written as

$$x_k = f(x_k) = (W_k^T D_k W_k)^{-1} W_k^T D_k t_k, \quad (16)$$

where  $D_k = \text{diag}([d_{\nu_1}, d_{\nu_2}, \dots, d_{\nu_l}])$  and

$$d_{\nu_i}(e_{i,k}) = \frac{\nu_i}{\nu_i \tau_i^2 + e_{i,k}^T e_{i,k}}. \quad (17)$$

---

**Algorithm 1** STKF

---

- 1: Step 1: Initialization
- 2: Choose  $\nu_i$  and  $\tau_i^2$  for channel  $i$ , maximum iteration number  $m_{\text{iter}}$ , and a threshold  $\varepsilon$ .
- 3: Step 2: State Prediction
- 4:  $\hat{x}_k^- = A\hat{x}_{k-1}^+$
- 5:  $P_k^- = AP_{k-1}^+A^T + Q_k$
- 6: Obtain  $B_p$  and  $B_r$  with  $B_pB_p^T = P_k^-$  and  $B_rB_r^T = R_k^*$
- 7: Obtain  $t_k$  and  $W_k$  through (13)
- 8: Step 3: State Update
- 9:  $\hat{x}_{k,0}^+ = \hat{x}_k^-$
- 10: while  $\frac{\|\hat{x}_{k,t}^+ - \hat{x}_{k,t-1}^+\|}{\|\hat{x}_{k,t}^+\|} > \varepsilon$  or  $t \leq m_{\text{iter}}$  do
  - 11:  $\hat{x}_{k,t}^+ = \hat{x}_k^- + \tilde{K}_{k,t}(y_k - C\hat{x}_k^-)$  ▷  $t$  starts from 1
  - 12:  $\tilde{K}_{k,t} = \tilde{P}_k^- C^T (C\tilde{P}_k^- C^T + \tilde{R}_k)^{-1}$
  - 13:  $\tilde{P}_k^- = B_p M_p^{-1} B_p^T$ ,  $M_p = \text{diag}(d_{\nu_i}(e_{1,k}), \dots, d_{\nu_i}(e_{n,k}))$
  - 14:  $\tilde{R}_k = B_r M_r^{-1} B_r^T$ ,  $M_r = \text{diag}(d_{\nu_i}(e_{n+1,k}), \dots, d_{\nu_i}(e_{n+m,k}))$
  - 15:  $e_{i,k} = t_{i,k} - w_{i,k} x_{k,t-1}^+$  ▷  $t_{i,k}$  is  $i$ -th element of  $t_k$
  - 16:  $t = t + 1$
- 17: end while
- 18:  $P_k^+ = (I - \tilde{K}_k C)P_k^- (I - \tilde{K}_k C)^T + \tilde{K}_k R_k \tilde{K}_k^T$

---

Note that the equation (16) can be regarded as the least square solution of (13) where  $E(\zeta_k^T \zeta_k) = D_k^{-1} = \text{diag}([\lambda_1, \lambda_2, \dots, \lambda_l])$  and

$$\lambda_i \triangleq d_{\nu_i}^{-1} = \underbrace{\tau_i^2}_{\text{constant}} + \underbrace{\frac{e_{i,k}^T e_{i,k}}{\nu_i}}_{\text{inflation}}. \quad (18)$$

We observe that both sides of (16) contain  $x_k$ , as  $e_k = t_k - W_k x_k$ . Then, it is natural to apply a fixed-point iteration for the solution of (16). Using a similar derivation as done in [6], we obtain the Student's  $t$ -based Kalman filter (STKF) summarized in Algorithm 1. Before giving the convergence condition of the fixed-point iteration in Line 10-17 in Algorithm 1, we provide the following lemma.

**Lemma 3** ([21]): The fixed-point algorithm (16) converges if  $\exists \gamma > 0$  and  $0 < \eta < 1$  such that the initial vector  $\|x_0\|_p < \gamma$ , and  $\forall x \in \{x \in \mathbb{R}^n : \|x\|_p \leq \gamma\}$ , the following holds (omitting time index  $k$  for simplicity)

$$\begin{cases} \|f(x)\|_p \leq \gamma, \\ \|\nabla_x f(x)\|_p \leq \eta, \end{cases} \quad (19)$$

where  $\|\cdot\|_p$  denotes an  $\ell_p$  norm of a vector or an induced norm of a matrix defined by  $\|A\|_p = \max_{\|x\|_p} \frac{\|Ax\|_p}{\|x\|_p}$  with  $p \geq 1$ , and  $\nabla_x f(x)$  is the Jacobian matrix of  $f(x)$ .

Denote the DOF vector as  $\nu = [\nu_1, \nu_2, \dots, \nu_l]^T \in \mathbb{R}^l$  and the unified DOF as  $\nu_1 = \nu_2 = \dots = \nu_l = \nu \in \mathbb{R}$ . The following Theorem 1 ensures the validity of first inequality in (19), while Theorem 2 guarantees the second one.

**Theorem 1:** In (16),  $\forall x \in \{x \in \mathbb{R}^n : \|x\|_1 \leq \gamma\}$ , it follows that  $\|f(x)\|_1 \leq \gamma$  if  $\gamma > \xi$  and  $\nu_i \geq \nu^*$  for  $i = 1, 2, \dots, l$ , where

$$\xi = \frac{\sqrt{n} \sum_{i=1}^l \frac{1}{\tau_i^2} |t_i| \|w_i^T\|_1}{\lambda_{\min}[\sum_{i=1}^l w_i^T w_i]},$$

and  $\nu^*$  is the solution of equation  $\phi(\nu) = \gamma$  with

$$\phi(\nu) = \frac{\sqrt{n} \sum_{i=1}^l |t_i| \|w_i^T\|_1}{\lambda_{\min} \left[ \sum_{i=1}^l d_{\nu}(\gamma \|w_i^T\|_1 + t_i) w_i^T w_i \right]}. \quad (20)$$

**Proof 4:** Denoting  $R_{ww} = W_k^T D_k W_k$  and  $R_{wt} = W_k^T D_k t_k$ , it follows that  $f(x) = R_{ww}^{-1} R_{wt}$  according to (16). Since the induced norm is compatible with vector  $\ell_p$  norm, we have

$$\|f(x)\|_1 = \|R_{ww}^{-1} R_{wt}\|_1 \leq \|R_{ww}^{-1}\|_1 \|R_{wt}\|_1. \quad (21)$$

According to matrix theory, we have

$$\begin{aligned}
\|R_{ww}^{-1}\|_1 &\leq \sqrt{n}\|R_{ww}^{-1}\|_2 = \sqrt{n}\lambda_{\max}[R_{ww}^{-1}] = \frac{\sqrt{n}}{\lambda_{\min}[R_{ww}]} \\
&= \frac{\sqrt{n}}{\lambda_{\min}[\sum_{i=1}^l w_i^T d_{\nu_i}(e_i) w_i]} \\
&\stackrel{(I)}{\leq} \frac{\sqrt{n}}{\lambda_{\min}[\sum_{i=1}^l w_i^T d_{\nu_i}(|t_i| + \gamma|w_i^T|_1) w_i]},
\end{aligned} \tag{22}$$

where (I) comes from  $|e_i| = |t_i - w_i x| \leq |t_i| + \gamma\|w_i\|_1$ . Furthermore, it holds that

$$\|R_{wt}\|_1 = \left\| \sum_i^l w_i^T d_{\nu_i}(e_i) t_i \right\|_1 \stackrel{(II)}{\leq} \sum_i^l \frac{1}{\tau_i^2} \|w_i^T\|_1 |t_i|, \tag{23}$$

where (II) comes from the fact  $d_{\nu_i}(e_i) \leq \frac{1}{\tau_i^2}$ . Substituting the expression of  $R_{ww}$  and  $R_{wt}$  into (21), one arrives

$$\|f(x)\|_1 \leq \phi(\nu) = \frac{\sqrt{n} \sum_i^l \frac{1}{\tau_i^2} \|w_i^T\|_1 |t_i|}{\lambda_{\min}[\sum_{i=1}^l w_i^T d_{\nu_i}(|t_i| + \gamma|w_i^T|_1) w_i]}. \tag{24}$$

In the case  $\nu_1 = \nu_2 = \dots = \nu_l = \nu$ ,  $\phi(\nu)$  degenerates to  $\phi(\nu)$  as follows:

$$\phi(\nu) = \frac{\sqrt{n} \sum_i^l |t_i| \|w_i^T\|_1}{\lambda_{\min} \left[ \sum_{i=1}^l d_{\nu}(\gamma\|w_i^T\|_1 + t_i) w_i^T w_i \right]}, \tag{25}$$

which is a decreasing function of  $\nu$ . Moreover, we have

$$\lim_{\nu \rightarrow \infty} \phi(\nu) = \xi = \frac{\sqrt{n} \sum_i^l \frac{1}{\tau_i^2} \|w_i^T\|_1 |t_i|}{\lambda_{\min}[\sum_{i=1}^l w_i^T w_i]}, \lim_{\nu \rightarrow 0^+} \phi(\nu) = \infty.$$

This indicates that if  $\gamma > \xi$ ,  $\phi(\nu) = \gamma$  always has a unique solution  $\nu^*$  over  $[0, \infty]$ . Subsequently, we consider a much more general case  $\nu_i \geq \nu^*$  for  $i = 1, 2, \dots, l$ . One observes that  $w_i^T d_{\nu_i}(|t_i| + \gamma|w_i^T|_1) w_i$  is a positive diagonal matrix and  $d_{\nu_i}(\cdot) \geq d_{\nu^*}(\cdot)$  if  $\nu_i \geq \nu^*$ . It follows that

$$\|f(x)\|_1 \leq \phi(\nu) \leq \phi(\nu^*) = \gamma.$$

This completes proof.

Theorem 2: In (16),  $\forall x \in \{x \in \mathbb{R}^n : \|x\|_1 \leq \gamma\}$ , it holds that  $\|f(x)\| \leq \gamma$ , and  $\|\nabla_x f(x)\| \leq \eta$  if

$$\gamma > \xi = \frac{\sqrt{n} \sum_i^l \frac{1}{\tau_i^2} \|w_i^T\|_1 |t(i)|}{\lambda_{\min} \left[ \sum_{i=1}^l w(i)^T w(i) \right]},$$

and  $\forall i$ ,  $\nu_i \geq \max\{\nu^*, \nu^+\}$ , where  $\nu^*$  is the solution of  $\phi(\nu) = \gamma$ , and  $\nu^+$  is the solution of  $\psi(\nu) = \eta$  ( $0 < \eta < 1$ ) with

$$\psi(\nu) = \frac{2\sqrt{n} \sum_i^l \frac{|t_i| + \gamma\|w_i^T\|_1}{\tau_i^4} \|w_i^T\|_1 (\gamma\|w_i^T w_i\|_1 + \|w_i^T t_i\|_1)}{\nu \lambda_{\min}[\sum_{i=1}^l w_i^T d_{\nu_i}(|t_i| + \gamma|w_i^T|_1) w_i]}. \tag{26}$$

Proof 5: To prove  $\|\nabla_x f(x)\| \leq \eta$ , it is sufficient to prove  $\forall j$ ,  $\|\frac{\partial}{\partial x_j}\|_1 \leq \eta$ . Based on the fact that

$$\frac{\partial \mathbf{U}^{-1}}{\partial \mathbf{x}} = -\mathbf{U}^{-1} \frac{\partial \mathbf{U}}{\partial \mathbf{x}} \mathbf{U}^{-1}, \quad \frac{\partial \mathbf{U} \mathbf{V}}{\partial \mathbf{x}} = \frac{\partial \mathbf{U}}{\partial \mathbf{x}} \mathbf{V} + \mathbf{U} \frac{\partial \mathbf{V}}{\partial \mathbf{x}}$$

where  $\mathbf{U}$  and  $\mathbf{V}$  are matrices and  $\mathbf{x}$  is a scalar, we have the following equation:

$$\begin{aligned}
\frac{\partial}{\partial x_j} f(x) &= \frac{\partial}{\partial x_j} R_{ww}^{-1} R_{wt} \\
&= -R_{ww}^{-1} \left[ \sum_{i=1}^l \frac{2\nu_i w_{i,j} e_i}{(\nu_i \tau_i^2 + e_i^T e_i)^2} w_i^T w_i \right] f(x) \\
&\quad + R_{ww}^{-1} \left[ \sum_{i=1}^l \frac{2\nu_i w_{i,j} e_i}{(\nu_i \tau_i^2 + e_i^T e_i)^2} w_i^T t_i \right],
\end{aligned} \tag{27}$$

where  $w_{i,j}$  is the  $j$ -th element of  $w_i$  and  $x_j$  is  $j$ -th element of vector  $x$ . Take one norm in both sides of (27), we have

$$\begin{aligned} \left\| \frac{\partial}{\partial x_j} f(x) \right\|_1 &\leq \left\| -R_{ww}^{-1} \left[ \sum_{i=1}^l \frac{2\nu_i w_{i,j} e_i}{(\nu_i \tau_i^2 + e_i^T e_i)^2} w_i^T w_i \right] f(x) \right\|_1 \\ &\quad + \left\| R_{ww}^{-1} \left[ \sum_{i=1}^l \frac{2\nu_i w_{i,j} e_i}{(\nu_i \tau_i^2 + e_i^T e_i)^2} w_i^T t_i \right] \right\|_1. \end{aligned} \quad (28)$$

For the first term on the right side of (28), we have

$$\begin{aligned} &\left\| -R_{ww}^{-1} \left[ \sum_{i=1}^l \frac{2\nu_i w_{i,j} e_i}{(\nu_i \tau_i^2 + e_i^T e_i)^2} w_i^T w_i \right] f(x) \right\|_1 \\ &\leq 2 \|R_{ww}^{-1}\|_1 \left\| \left[ \sum_{i=1}^l \frac{\nu_i w_{i,j} e_i}{(\nu_i \tau_i^2 + e_i^T e_i)^2} w_i^T w_i \right] \right\|_1 \|f(x)\|_1 \\ &\stackrel{(I)}{\leq} 2\gamma \|R_{ww}^{-1}\|_1 \sum_{i=1}^l \left\| \frac{\nu_i w_{i,j} e_i}{(\nu_i \tau_i^2 + e_i^T e_i)^2} w_i^T w_i \right\|_1 \\ &\stackrel{(II)}{\leq} 2\gamma \|R_{ww}^{-1}\|_1 \sum_{i=1}^l \frac{|t_i| + \gamma \|w_i^T\|_1}{\nu_i \tau_i^4} \|w_i^T\|_1 \|w_i^T w_i\|_1, \end{aligned} \quad (29)$$

where (I) comes from the convexity of vector  $\ell_1$  norm and  $f(x) \leq \gamma$ , and (II) comes from  $|w_{i,j} e_i| \leq (|t_i| + \gamma \|w_i\|_1) \|w_i^T\|_1$  and  $\frac{\nu_i}{(\nu_i \tau_i^2 + e_i^T e_i)^2} \leq \frac{1}{\nu_i \tau_i^4}$ . Similarly, we have

$$\begin{aligned} &\left\| R_{ww}^{-1} \left[ \sum_{i=1}^l \frac{2\nu_i w_{i,j} e_i}{(\nu_i \tau_i^2 + e_i^T e_i)^2} w_i^T t_i \right] \right\|_1 \\ &\leq 2 \|R_{ww}^{-1}\|_1 \sum_{i=1}^l \frac{|t_i| + \gamma \|w_i^T\|_1}{\nu_i \tau_i^4} \|w_i^T\|_1 \|w_i^T t_i\|_1. \end{aligned} \quad (30)$$

Substituting (22), (29), and (30) into (28), we obtain

$$\begin{aligned} &\left\| \frac{\partial}{\partial x_j} f(x) \right\|_1 \leq \psi(\boldsymbol{\nu}) \\ &= \frac{2\sqrt{n} \sum_{i=1}^l \frac{|t_i| + \gamma \|w_i^T\|_1}{\nu_i \tau_i^4} \|w_i^T\|_1 (\gamma \|w_i^T w_i\|_1 + \|w_i^T t_i\|_1)}{\lambda_{\min} [\sum_{i=1}^l w_i^T d_{\nu_i}(|t_i| + \gamma \|w_i^T\|_1) w_i]}. \end{aligned} \quad (31)$$

By setting  $\nu_i = \nu$  for all  $i$ , the function  $\psi(\boldsymbol{\nu})$  degenerates to  $\psi(\nu)$  which is a function with respect to  $\nu$  as follows:

$$\psi(\nu) = \frac{2\sqrt{n} \sum_{i=1}^l \frac{|t_i| + \gamma \|w_i^T\|_1}{\nu_i \tau_i^4} \|w_i^T\|_1 (\gamma \|w_i^T w_i\|_1 + \|w_i^T t_i\|_1)}{\lambda_{\min} [\sum_{i=1}^l w_i^T d_{\nu_i}(|t_i| + \gamma \|w_i^T\|_1) w_i]} \quad (32)$$

In such cases, one has

$$\left\| \frac{\partial}{\partial x_j} f(x) \right\|_1 \leq \psi(\nu). \quad (33)$$

One can see that (33) is a continuous and monotonically decreasing function satisfying  $\lim_{\nu \rightarrow 0^+} \psi(\nu) = \infty$  and  $\lim_{\nu \rightarrow \infty} \psi(\nu) = 0$ . This implies that  $\psi(\nu) = \eta$  has a unique solution  $\nu^+$  and  $\psi(\nu) \leq \eta$  if  $\nu \geq \nu^+$ . Observing (31) and (33), we have  $\psi(\boldsymbol{\nu}) \leq \psi(\nu^+)$  if  $\nu_i \geq \nu^+$  for all  $i$ . This indicates that  $0 < \psi(\boldsymbol{\nu}) \leq \eta$  if  $\forall i, \nu_i \geq \nu^+$ . This completes the proof.

Remark 2: Theorems 1 and 2 provide a sufficient condition for the convergence of the fix-point iteration (16) under dynamics (13) and loss (14).

We further extend Theorems 1 and 2 to a general loss  $J_{\boldsymbol{\nu}}(e; \boldsymbol{\nu}, \boldsymbol{\tau}^2) = \sum_{i=1}^l J_{\nu_i}(e_i; \nu_i, \tau_i^2)$  where  $\nu_i > 0$  and  $\tau_i^2 > 0$  are the hyperparamters and  $e_i \in \mathbb{R}$  is the  $i$ -th element of  $e$ . By denoting  $\frac{\partial J_{\nu_i}}{\partial e_i} = d_{\nu_i}(e_i) e_i$  and  $\frac{\partial d_{\nu_i}(e_i)}{\partial e_i} = \iota_{\nu_i}(e_i) e_i$ , Theorem 3 provide a necessary condition for the convergence of a general loss using a fixed-point solution.

Theorem 3: Considering dynamics (13), a general loss  $J_{\boldsymbol{\nu}}(e; \boldsymbol{\nu}, \boldsymbol{\tau}^2) = \sum_{i=1}^l J_{\nu_i}(e_i; \nu_i, \tau_i^2)$  can be solved by a fixed-point algorithm with guaranteed convergence if the following conditions are fulfilled:

- Condition 1:  $J_{\nu_i}(e_i)$  is a non-decreasing continuous function with respect to  $|e_i|$  and gives its minimum at  $e_i = 0$ .
- Condition 2:  $\exists \kappa \in \mathbb{R}^+$  so that  $0 \leq d_{\nu_i}(e_i) \leq \kappa$ . Moreover,  $d_{\nu_i}(e_i)$  is an increasing function of  $\nu_i$  with  $\lim_{\nu_i \rightarrow 0^+} d_{\nu_i}(e_i) = 0$  for any  $|e_i| > 0$ .
- Condition 3:  $\iota_{\nu_i}(e_i)$  is bounded for any  $e_i$ .

TABLE I  
Some Robust Losses Fulfilling Theorem 3.

$J_\nu(e)$	$d_\nu(e)$	$\iota_\nu(e)$	special cases
$\frac{\nu}{2} \log \left(1 + \frac{e^2}{\nu \tau^2}\right), \nu \in (0, \infty)$	$\frac{\nu}{\nu \tau^2 + e^2}$	$-\frac{2\nu}{(\nu \tau^2 + e^2)^2}$	$\lim_{\nu \rightarrow \infty} J_\nu(e) = \frac{e^2}{2\tau^2}$
$\nu^2 \left(1 - \exp\left(-\frac{e^2}{2\nu^2 \tau^2}\right)\right), \nu \in (0, \infty)$	$\frac{1}{\tau^2} \exp\left(-\frac{e^2}{2\nu^2 \tau^2}\right)$	$-\frac{1}{\nu^2 \tau^4} \exp\left(-\frac{e^2}{2\nu^2 \tau^2}\right)$	$\lim_{\nu \rightarrow \infty} J_\nu(e) = \frac{e^2}{2\tau^2}$
$\frac{2-\nu}{\nu} \left(\left(\frac{e^2/\tau^2}{2-\nu} + 1\right)^{\nu/2} - 1\right), \nu \in (0, 2)$	$\frac{1}{\tau^2} \left(\frac{e^2/\tau^2}{2-\nu} + 1\right)^{\nu/2-1}$	$-\frac{1}{2\tau^4} \left(\frac{e^2/\tau^2}{2-\nu} + 1\right)^{\nu/2-2}$	$\lim_{\nu \rightarrow 2} J_\nu(e) = \frac{e^2}{2\tau^2}$
$\sqrt{\nu(\nu + e^2/\tau^2)} - \nu, \nu \in (0, \infty)$	$\frac{1}{\tau^2 \sqrt{1 + \frac{e^2}{\nu \tau^2}}}$	$-\frac{1}{\nu \tau^4} \left(1 + \frac{e^2}{\nu \tau^2}\right)^{-3/2}$	$\lim_{\nu \rightarrow \infty} J_\nu(e) = \frac{e^2}{2\tau^2}$

TABLE II  
Computational Complexity of Algorithm 1.

Lines or equations	Absolute value, addition/subtraction, and multiplication	matrix inversion, division, Cholesky decomposition
Line 4	$2n^2 - n$	0
Line 5	$4n^3 - n^2$	0
Line 6	0	$O(n^3) + O(m^3)$
Line 7	$2m^2n + 2n^2 + 2m^2 - nm - n - m$	$O(m^3) + O(n^3)$
Line 11	$4nm$	0
Line 12	$4n^2m + 4m^2n - 3nm$	$O(m^3)$
Line 13	$2n^3 + 2n$	$n + n$
Line 14	$2m^3 + 2m$	$m + m$
Line 15	$2n^2 + 2nm$	0
Line 18	$4n^3 + 4n^2m - 2n^2 + 2nm^2$	0

- Condition 4:  $\nu_i > \max\{\nu^*, \nu^+\}$  for  $i = 1, 2, \dots, l$ , where  $\nu^*$  and  $\nu^+$  are constants determined analogously to the expressions in (20) and (26), respectively.

Proof 6: One observes that Condition 1 ensures that  $J_\nu(e)$  is a well-defined loss function. Condition 2 guarantees the validity of (24). Condition 3 guarantees the validity of (30). Condition 4 (combined with the above three conditions) guarantees the hold of the inequality in (19) by analogy with the proof of Theorems 1 and 2. This completes the proof.

Some exemplary losses  $J_\nu(e; \nu, \tau^2) = \sum_{i=1}^l J_{\nu_i}(e_i; \nu_i, \tau_i^2)$  are listed in Table I. For simplicity, we use  $l = 1$  so the subscript  $i$  is omitted. We find that the proposed STKF uses the logarithmic loss for algorithm derivation while the MKCKF [15] and AORSE-sqrt algorithm [18] utilize the exponential loss and square root loss as optimization objectives, respectively (these three estimators correspond to the first three losses in Table I). It is worth mentioning that a different robust filter can be obtained by simply replacing the expression of  $d_{\nu_i}(e_{i,k})$  Lines 13 and 14 with the expressions in Table I (the second column) in Algorithm 1, which greatly simplify the algorithm design.

Proposition 1: The STKF, MKCKF [15], and AORSE-sqrt [18] are identical to the standard KF [36] as  $\nu_i \rightarrow \infty$  for  $i = 1, 2, \dots, l$ .

Proof 7: Note that STKF, MKCKF, and AORSE-sqrt can be obtained by substituting the expression of  $d_{\nu_i}$  in Lines 13 and 14 of Algorithm 1 with the first, second, and third entries in Table I, respectively. In the case that  $\nu_i \rightarrow \infty$  for  $i = 1, 2, \dots, l$ , we have

$$\begin{aligned}
 \lim_{\nu_i \rightarrow \infty} \frac{\nu_i}{\nu_i \tau_i^2 + e^2} &= 1, \\
 \lim_{\nu_i \rightarrow \infty} \frac{1}{\tau_i^2} \exp\left(-\frac{e^2}{2\nu_i^2 \tau_i^2}\right) &= 1, \\
 \lim_{\nu_i \rightarrow \infty} \frac{1}{\tau_i^2 \sqrt{1 + \frac{e^2}{\nu_i \tau_i^2}}} &= 1.
 \end{aligned} \tag{34}$$

It follows  $M_p = I$  and  $M_r = I$  of the appreciate dimension in Algorithm 1, making it identical to the KF. This completes the proof

## B. Algorithm Complexity

The main computational complexity of the STKF is summarized in Table II. By assuming the average iteration number for the while loop in Algorithm 1 is  $\bar{t}$ , one has

$$\begin{aligned} S_{our} = & [8n^3 + 2n^2 + 4n^2m - 2n + 4m^2 + 2m^2n + nm + 2nm^2 \\ & - m + 2O(n^3) + 2O(m^3)] + \bar{t}[2m^3 + 2n^3 + 2n^2 + 4n^2m \\ & + 4m^2n + 3mn + 4n + 4m + O(m^3)]. \end{aligned} \quad (35)$$

As a comparison, the complexity of KF has

$$S_{kf} = 6n^3 + 6n^2m + 4m^2n + mn - n + O(m^3). \quad (36)$$

One can see that the complexity of the STKF is moderate compared with KF. In practical implementations, the fixed-point algorithm typically converges after 2-3 iterations.

## C. Connection with Adaptive Filter

The adaptive filters, governing by linear equation (13), estimate both the state  $x_k$  and covariance  $R_{\zeta_k \zeta_k^T}$  as follows:

$$\{\hat{x}_k, \hat{R}_{\zeta_k \zeta_k^T}\} = \arg \max J(x_k, R_{\zeta_k \zeta_k^T} | t_k), \quad (37)$$

where  $J(\cdot)$  is a loss function,  $R_{\zeta_k \zeta_k^T}$  is the noise covariance, and  $t_k$  is the current measurement. The following theorem builds a connection between STKF and VBKF [24].

Theorem 4: Given dynamics (13), the STKF derived from Student's  $t$ -distribution with hyper-parameters  $\nu_i$  and  $\tau_i^2$  is identical to VBKF [24] with fixed prior distributions Inv-Gam  $(\lambda_i | \frac{\nu_i}{2}, \frac{\nu_i \tau_i^2}{2})$ .

Proof 8: According to (13), using the inverse-Gamma distribution as the a priori distribution of covariance, we have

$$\begin{aligned} p(x_k, R_{\zeta_k \zeta_k^T} | t_k) &= p(x_k | t_k, R_{\zeta_k \zeta_k^T}) p(R_{\zeta_k \zeta_k^T}) \\ &= \prod_{i=1}^l \frac{1}{\sqrt{2\pi\lambda_i}} \exp\left(-\frac{1}{2} \frac{(t_i - w_i x_k)^2}{\lambda_i}\right) \\ &\cdot \frac{(\nu_i \tau_i^2 / 2)^{\nu_i/2}}{\Gamma(\nu_i/2)} \lambda_i^{-(\nu_i/2+1)} \exp\left(-\frac{\nu_i \tau_i^2}{2\lambda_i}\right) \\ &\propto \prod_{i=1}^l \lambda_i^{-\frac{\nu_i+3}{2}} \exp\left(-\frac{\nu_i \tau_i^2}{2\lambda_i}\right) \exp\left(-\frac{1}{2} \frac{e_i^2}{\lambda_i}\right), \end{aligned} \quad (38)$$

where  $\lambda_i$  denotes the covariance for  $e_i = t_i - w_i x_k$ . Note that (38) has the same expression with the approximated conditional distribution described in VBKF. Based on maximum a posteriori (MAP) principle, the objective function can be written as

$$\begin{aligned} J &= -\log p(x_k, R_{\zeta_k \zeta_k^T} | t_k) \\ &\propto \sum_{i=1}^l \left[ \left( \frac{\nu_i + 3}{2} \right) \log(\lambda_i) + \frac{\nu_i \tau_i^2}{2\lambda_i} + \frac{(t_i - w_i x_k)^2}{2\lambda_i} \right]. \end{aligned} \quad (39)$$

Letting  $\frac{\partial J}{\partial \lambda_i} = 0$  gives

$$\lambda_i = \frac{\nu_i \tau_i^2 + (t_i - w_i x_k)^2}{\nu_i + 3}.$$

Substituting this expression back into  $J$  and ignoring terms that are not relevant to  $x_k$  gives

$$\begin{aligned} J &= \sum_{i=1}^l \left[ \left( \frac{\nu_i + 3}{2} \right) \log(\nu_i \tau_i^2 + (t_i - w_i x_k)^2) \right. \\ &\quad \left. - \left( \frac{\nu_i + 3}{2} \right) \log(\nu_i + 3) + \frac{\nu_i + 3}{2} \right] \\ &\propto \sum_{i=1}^l \left( \frac{\nu_i + 3}{2} \right) \log(\nu_i \tau_i^2 + e_i^2) \\ &\propto \sum_{i=1}^l \left( \frac{\nu_i + 3}{2} \right) \log\left(1 + \frac{e_i^2}{\nu_i \tau_i^2}\right), \end{aligned} \quad (40)$$

which is a weighted form of (14). According to Lemma 2, under the statically independent assumption, (40) can be equivalently written as

$$J \propto \sum_{i=1}^l \left( \frac{\nu_i}{2} \right) \log \left( 1 + \frac{e_i^2}{\nu_i \tau_i^2} \right), \quad (41)$$

which is the standard student's  $t$ -distribution induced loss function. This indicates that the two filters, STKF and VBKF with fixed prior distributions, are identical since they share the same loss functions. This completes the proof. Theorem 4 builds a bridge between adaptive filtering and robust filtering, i.e., in our context, robust filtering can be regarded as a special case of adaptive filtering with fixed prior distribution parameters. A similar assertion is vaguely hinted at Chapter 5.5.3 of [36], but without a rigorous proof.

Remark 3: A by-product of Theorem 4 is that, instead of solving (39) using a set of coupled equations as shown in [24], we solve the problem subsequently: (1) estimate the state using a fix-point iteration; (2) update the loss hyper-parameters and posterior error covariance (see Algorithm 2 and numerical simulations in IV-A for details). The two paths give the identical results, but our method possesses some advantages: On the one hand, it decouples the “robustness process” and “adaptive process”, allowing us to design switching rules for complex noise scenarios. On the other hand, the decoupled method reduces algorithm complexity by calculating the posterior error covariance only once, rather than  $N$  times as shown in [24]. The fixed-point iteration with break conditions is summarized in Lines 10 to 17 in Algorithm 1, which is preferable compared with the fixed iteration number  $N$  in [24], see the demonstration in the last column of Table III.

#### D. Robust Adaptive Filtering

According to Lemma 1 and Theorem 4, we have the insights that optimizing (14) actually jointly optimizes the state and covariance, where the diagonal element of the variance follows an inverse-Gamma distribution, which can be obtained by a fixed-point iteration as shown in Line 8-17 in Algorithm 1. We then focus on the update of hyper-parameter  $\nu_i$  and  $\tau_i^2$ . Based on the variational inference [24], [33], when applying (3) as a conjugate prior distribution, the posterior hyper-parameters should be updated as

$$\begin{aligned} \nu_{i,k}^+ &= \nu_{i,k}^- + 1, \\ \tau_{i,k}^2 &= (\tau_{i,k}^2)^- + \frac{e_{i,k}^T e_{i,k}}{\nu_{i,k}^+} + \frac{[W_k P_k W_k]_{ii}}{\nu_{i,k}^+}, \end{aligned} \quad (42)$$

where  $P_k$  is the posterior error covariance and  $[*]_{ii}$  denotes the  $i$ -th diagonal element of matrix  $*$ . The proof of (42) is available in Appendix VI-B. One observes that the update of  $\nu_i$  is not related with the error  $e_{i,k}$ . In the iterative filtering, it is natural to assume that the hyper-parameter at the next time step is identical to the previous ones. However, this would induce unbounded  $\nu_{i,k}^+$  and  $\tau_{i,k}^2$ . To alleviate this problem, we employ a forgetting factor  $\rho_i \in (0, 1)$  for channel  $i$  in the hyper-parameter prediction step, which is motivated by [24] and given as follows:

$$\begin{aligned} \nu_{i,k}^- &= \rho_i \nu_{i,k-1}^+ + 1, \\ (\tau_{i,k}^2)^- &= \rho_i (\tau_{i,k-1}^2)^+, \\ \nu_{i,k}^+ &= \nu_{i,k}^-. \end{aligned} \quad (43)$$

Combining (42) and (43), in the hyper-parameter update step, one has

$$(\tau_{i,k}^2)^+ = (\tau_{i,k}^2)^- + \frac{e_{i,k}^T e_{i,k}}{\nu_{i,k}^+} + \frac{[W_k P_k W_k]_{ii}}{\nu_{i,k}^+}. \quad (44)$$

In the extreme case  $\rho = 1$ , the hyper-parameter update should be halted, which gives the following update:

$$\nu_{i,k}^+ = \nu_{i,k-1}^+, \quad (\tau_{i,k}^2)^+ = (\tau_{i,k-1}^2)^- = (\tau_{i,k-1}^2)^+. \quad (45)$$

We name the new algorithm STKF-AR1 and provide a summary of it in Algorithm 2.

Proposition 2: The STKF-AR1 is equivalent to the STKF when  $\rho_i = 1$  for all  $i = 1, 2, \dots, l$ . Additionally, it becomes identical to the VBKF (with forgetting factor  $\rho_c$ ) when  $\rho_i = 1$  and  $\nu_i \rightarrow \infty$  for  $i = 1, 2, \dots, n$  and  $\rho_j = \rho_c$  for  $j = n+1, n+2, \dots, l$ , where  $0 < \rho_c < 1$  is a scalar.

The proof of the proposition is available in Appendix VI-C.

Remark 4: The proposed STKF-AR1 is much more powerful than the robust filter (STKF) and adaptive filter (VBKF) since it combines them both. Specifically, VBKF degenerates significantly with adaptive process noise and with the existence of outliers in the process noise, which can be addressed effectively in STKF-AR1 since STKF-AR1 has the ability to address either outliers or adaptive noise at different channels by assigning proper  $\rho_i$ , see its performance in simulations in Section IV-C.

---

**Algorithm 2 STKF-AR1**


---

- 1: Initialization
- 2: Choose  $\nu_i$  and  $\tau_i^2$  for channel  $i$ , maximum iteration number  $m_{\text{iter}}$ , and a threshold  $\varepsilon$ .
- 3: State Prediction
- 4: Run Line 4 to 7 in Algorithm 1.
- 5: Hyper-parameter Prediction
- 6: for  $i = 1$  to  $l$  do
- 7:   if  $0 < \rho_i < 1$  then
- 8:     Execute (43) to obtain  $v_{i,k}^+$  and  $(\tau_{i,k}^2)^-$
- 9:   else if  $\rho_i = 1$  then
- 10:     Execute (45) to obtain  $v_{i,k}^+$  and  $(\tau_{i,k}^2)^-$
- 11:   end if
- 12: end for
- 13: State Update
- 14: Run Line 8-17 in Algorithm 1 to obtain  $\hat{x}_k$  and  $P_k$
- 15: Hyper-parameter Update
- 16: for  $i = 1$  to  $l$  do
- 17:   if  $0 < \rho_i < 1$  then
- 18:     Execute (44) to update  $(\tau_{i,k}^2)^+$
- 19:   else if  $\rho_i = 1$  then
- 20:     Execute (45) to update  $(\tau_{i,k}^2)^+$
- 21:   end if
- 22: end for

---

**Algorithm 3 STKF-AR2**


---

- 1: Run Line 1 to 14 in Algorithm 2
- 2: Hyper-parameter Update
- 3: for  $i = 1$  to  $l$  do
- 4:   if  $0 < \rho_i < 1$  then
- 5:     Execute (44) to obtain  $(\tau_{i,k}^2)^+$
- 6:     if  $|(\tau_{i,k}^2)^+ - (\tau_{i,k}^2)^-| > \xi$  then
- 7:       Revert the update by  $(\tau_{i,k}^2)^+ = (\tau_{i,k-1}^2)^+$
- 8:     end if
- 9:   else if  $\rho_i = 1$  then
- 10:     Execute (45) to update  $(\tau_{i,k}^2)^+$
- 11:   end if
- 12: end for

---

We then consider the case that the noise variance is time-varying and is occasionally polluted by outliers. To avoid the harmful effects of outliers on the adaptive mechanism, we design a switching rule. Specifically, we compare the obtained variance  $(\tau_{i,k}^2)^+$  with expected one  $(\tau_{i,k}^2)^-$ , if the difference  $|(\tau_{i,k}^2)^+ - (\tau_{i,k}^2)^-| \leq \xi$ , we recognize current noise as normal noise. Then we update  $\tau_{i,k}^2$  as shown in (44). In the case that  $|(\tau_{i,k}^2)^+ - (\tau_{i,k}^2)^-| > \xi$ , we recognize the current noise as a outlier. Correspondingly, we keep the expected variance and  $\tau_{i,k}^2$  unchanged as shown in (45).

A remaining question is the selection of  $\xi$ . According to inverse-Gamma distribution in (3) and Laplace's approximation, one has  $\text{Inv-Gam}(\lambda | \frac{\nu}{2}, \frac{\nu\tau^2}{2})|_{\lambda=\frac{\nu\tau^2}{\nu+1}} \sim \mathcal{N}(\mu, \sigma^2)$  where  $\mu = \tau^2$  and  $\sigma^2 = \frac{2\nu^2\tau^4}{(\nu+1)^3}$  when applying Laplace approximation at point  $\lambda = \frac{\nu\tau^2}{\nu+1}$  (see Appendix VI-D). Hence, we advise setting  $\xi = \eta\sqrt{\frac{2\nu^2}{(\nu+1)^3}}\tau^2$  where  $\eta \in [0.25, 1]$ , corresponding to  $\pm\eta\sigma$  region of the approximated distribution. We name the new algorithm as STKF-AR2 and it is summarized in Algorithm 3.

#### E. Convergence Rate Analysis of the Unknown Covariance

Analyze the convergence speed of (44) directly is difficult due to the complex coupling between the unknown covariance and the state. Instead, we focus on the steady state behavior of  $(\tau_{i,k}^2)^+$ . Based on (43), when  $\nu_i$  is steady, one has

$$\nu_{i,\infty}^+ = \rho_i \nu_{i,\infty}^+ + 1.$$

It follows that

$$\nu_{i,\infty}^+ \triangleq \nu_i = \frac{1}{1 - \rho_i}. \quad (46)$$

Denoting  $\lambda_{i,k}^+ \triangleq (\tau_{i,k}^2)^+$  and substituting the expression of (46) into (44) obtains

$$\lambda_{i,k}^+ = \rho_i \lambda_{i,k-1}^+ + (1 - \rho_i) e_{i,k}^T e_{i,k} + (1 - \rho_i) w_{i,k} P_k w_{i,k}^T, \quad (47)$$

where  $e_{i,k} = t_{i,k} - w_{i,k} \hat{x}_k$ ,  $w_{i,k}$  is the  $i$ -th row of  $W$ , and  $P_k = E(\tilde{x}_k \tilde{x}_k^T)$  is the posterior error covariance with  $\tilde{x}_k = x_k - \hat{x}_k$  denoting the estimation error. Assuming  $\zeta_{i,k} = t_{i,k} - w_{i,k} x_k \sim \mathcal{N}(0, \Sigma_k^g)$  ( $\zeta_{i,k}$  is the  $i$ -th element of  $\zeta_k$  as shown in (13)), it follows that  $e_{i,k} = \zeta_{i,k} + w_{i,k} \tilde{x}_k$  and  $E(e_{i,k}^T e_{i,k}) \triangleq \Sigma_k = \Sigma_k^g + w_{i,k} P_k w_{i,k}^T$ . Then, we have the following theorem.

**Theorem 5:** As  $k \rightarrow \infty$ , one has  $E(\lambda_k^+) = \bar{\Sigma}_k$  and  $\text{Var}(\lambda_k^+) = \frac{2(1-\rho_i)\Sigma_k^2}{1+\rho_i}$  where  $\bar{\Sigma}_k = \Sigma_k^g + 2w_{i,k} P_k w_{i,k}^T$  and  $\Sigma_k = \Sigma_k^g + w_{i,k} P_k w_{i,k}^T$ .

**Proof 9:** Taking expectation on both side of (47), one has

$$\begin{aligned} E(\lambda_{i,k}^+) &= \rho_i E(\lambda_{i,k-1}^+) + (1 - \rho_i) E(e_{i,k}^T e_{i,k}) \\ &\quad + (1 - \rho_i) E(w_{i,k} P_k w_{i,k}^T). \end{aligned} \quad (48)$$

It follows that, as  $k \rightarrow \infty$ ,

$$E(\lambda_{i,k}^+) = E(e_{i,k}^T e_{i,k}) + w_{i,k} P_k w_{i,k}^T = \Sigma_k^g + 2w_{i,k} P_k w_{i,k}^T.$$

The recursive variance follows

$$\text{Var}(\lambda_{i,k}^+) = \rho_i^2 \text{Var}(\lambda_{i,k-1}^+) + (1 - \rho_i)^2 \text{Var}(e_{i,k}^T e_{i,k}). \quad (49)$$

We know that  $\text{Var}(e_{i,k}^T e_{i,k}) = 2\Sigma_k^2$ . Hence, the steady state variance converges to

$$\text{Var}(\lambda_{i,k}^+) = \frac{2(1 - \rho_i)\Sigma_k^2}{1 + \rho_i}.$$

This completes the proof.

**Remark 5:** The above theorem demonstrates that the expectation of  $\lambda_{i,k}^+$  converges to  $\bar{\Sigma}_k$  with variance  $\frac{2(1-\rho_i)\Sigma_k^2}{1+\rho_i}$  at the steady state. Note that  $\Sigma_k \geq \Sigma_k^g$ , which implies that the proposed method is overestimated. However, this is generally not a concern since  $P_k$  is negligible compared with  $\Sigma_k^g$  in most situations.

We then analyze the transient behavior of  $E(\lambda_{i,k}^+)$ . Without loss of generality, we assume that the noise variance follows a step-like signal at time step  $m$ , i.e.,

$$E(\zeta_{i,k}^T \zeta_{i,k}) = \begin{cases} \Sigma_1^g, & \text{if } k < m, \\ \Sigma_2^g, & \text{if } k \geq m. \end{cases} \quad (50)$$

It is worth noting that the statistics of  $e_{i,k}$  is related with both  $\zeta_{i,k}^g$  and  $\tilde{x}_k$ . To simplify the analysis, we give the following assumptions.

**Assumption 1:** The state error covariance and the expectation of the unknown variance have converged to their steady states at time step  $m-1$ , i.e.,  $E(\tilde{x}_{m-1}^T \tilde{x}_{m-1}) = P_{m-1} \triangleq P_1$  and  $E(\lambda_{i,m-1}^+) \triangleq \bar{\Sigma}_1 = \Sigma_1^g + 2w_{i,j-1} P_1 w_{i,j-1}^T$ .

**Assumption 2:** We assume that the state error covariance converges to its steady state immediately after the noises covariance jumping, i.e.,  $E(\tilde{x}_m^T \tilde{x}_m) = P_m \triangleq P_2$  where  $P_2$  is the steady state error covariance.

Assumption 2 simplifies the analysis of the convergence behavior of  $E(\lambda_{i,k}^+)$  for  $k \geq m$ . It is also worth mentioning that, in many applications, the magnitude of the error covariance is neglectable compared with measurement noise covariance, resulting in a simplified convergence behavior analysis for  $\lambda_{i,k}$ . Denote  $\Sigma_2 \triangleq \Sigma_2^g + w_{i,j-1} P_2 w_{i,j-1}^T$  and  $\bar{\Sigma}_2 \triangleq \Sigma_2^g + 2w_{i,j-1} P_2 w_{i,j-1}^T$ . According to Theorem 5 and Assumptions 1 and 2, we have the following theorem.

**Theorem 6:** Given (50) and Assumptions 1 and 2, the noise variance estimation error  $\delta_{p,i}$  decays exponentially with rate  $\rho_i$  and time constant  $\tau_i = -\frac{1}{\ln \rho_i}$  (see the time constant definition in [37]), i.e.,

$$\delta_{p,i} = \delta_0 \rho_i^p, \quad p = k - m + 1 \geq 1, \quad (51)$$

where  $\delta_0 = \bar{\Sigma}_2 - \bar{\Sigma}_1$  is the initial error and  $\delta_{p,i} \triangleq E(\lambda_{i,k}^+) - \bar{\Sigma}_2$  is the estimation error.

**Proof 10:** According the (48) and the definition of  $\delta_{p,i}$ , it follows that

$$\delta_{p,i} + \bar{\Sigma}_2 = \rho_i (\delta_{p-1,i} + \bar{\Sigma}_2) + (1 - \rho_i) (\Sigma_2 + w_{i,k} P_2 w_{i,k}^T).$$

According to the definition of  $\Sigma_2$  and  $\bar{\Sigma}_2$ , we have  $\bar{\Sigma}_2 = \Sigma_2 + w_{i,k} P_2 w_{i,k}^T$ . Thus, we have

$$\delta_{p,i} = \rho_i \delta_{p-1,i},$$

and hence one obtains (51) under step-like variance. According to the definition of time constant [37], it follows that  $\tau_i = -\frac{1}{\ln \rho_i}$ . This completes the proof.

#### F. Parameter Selection and Discussion

There are three types of parameters in our proposed algorithms: the DOF  $\nu_i$ , the scale parameter  $\tau_i^2$ , and the decay coefficient  $\rho_i$ . The former two parameters are closely related to statistical characteristics of  $i$ -th channel of  $\zeta_k$  as shown in (13). Since the nominal covariance  $E(\zeta_k \zeta_k^T) = I$ , we can use  $\tau_i^2 = 1$  for the three proposed algorithms. As for the  $\nu_i$ , in robust filters as given in Algorithm 1, it reflects how confidence we are about our nominal covariance (see Remark 1) and a smaller value is preferred in situations with high probability of outliers. This conclusion can also be implicitly verified by (18), where it is observed that the temporary variance increases as  $\nu_i$  decreases (with  $\nu_i > 0$ ), indicating an enhanced ability to handle outliers, at the price of degenerated ability on Gaussian noise. In terms of implications, we recommend using  $\nu_i \rightarrow \infty$  for channels with Gaussian noise, and applying  $\nu_i \in [0.1, 5]$  for channels that may be contaminated by outliers.

The selection of  $\rho_i$  is paramount in the adaptive filter and adaptive-robust filter (i.e., Algorithms 2 and 3), but is not rarely discussed in the literature. According to variational inference, the DOF  $\nu_{i,k}$  keeps increasing with  $k$  according to (42), which would destroy the adaptive mechanism as  $\nu_{i,k} \rightarrow \infty$  recovers the KF. Hence, a decay coefficient  $\rho_i$  is indispensable which balance the convergence speed and the smoothness of the variance estimation, as details given in Theorems 5 and 6. In implications, we advise using  $\rho_i \in [0.95, 1)$ . In the case  $\rho_i = 1$  for all channels, the proposed Algorithm 2 recovers the STKF and it becomes identical to KF if we further set  $\nu_i \rightarrow \infty$  for all channels.

We reveal that the robustness and adaptability are two competing goals. As in robust filter, we stubbornly keep the prior variance  $\tau_{i,k}^2$  fixed and estimate the latent variance  $\lambda_{i,k}$  temporarily by applying (18). On the contrary, we continually update our prior variance  $\tau_{i,k}^2$  in adaptive filter according to (44). The philosophy behind robustness is based on the idea that outliers are rare and exceptional, while the concept of adaptability stems from the understanding that noise patterns are constantly changing, making them incompatible in one unified framework. To handle situations of adaptive noises with occasionally outliers, a switching rule is designed and the threshold  $\xi$  controls the boundary of robustness and adaptability. Our Algorithm 3 (STKF-AR2) recovers the STKF-AR1 when applying  $\xi = 0$ .

This work provides a unified framework that incorporates conventional KF, robust filter, adaptive filter, as well as robust-adaptive filter, by tuning hyperparameters. We want to stress that our proposed framework is channel level (i.e., we can select different  $\nu_i$  for different channels) and incorporates both process noise and measurement noise adaptation and/or robustness, which is a unique advantage and allows practitioners to incorporate their prior knowledge on the noise characteristics into the algorithm design. For example, if we know that the process noise is occasionally contaminated by outliers, while the measurement noise covariance is time-varying, we can assign small fixed values to the corresponding  $\nu_i$  for the process channels and apply the adaptive mechanism to the measurement channels. More comprehensive comparisons of different estimators are available in simulations.

## IV. Simulations

In this section, we demonstrate the identity of STKF and VBKF with a fixed prior distribution, as well as the equivalence of STKF-AR1 (under certain hyperparameters) and VBKF, in Example 1. Subsequently, we visualize the trade-off between unknown covariance tracking speed and tracking variance in Example 2. Finally, we demonstrate the effectiveness of the proposed approaches in complex noise scenarios in Example 3. The codes are online available at <https://github.com/lsl-zsj/Variational-Robust-Kalman-Filters>.

#### A. Example 1: Identity Property

We consider the following tracking problem:

$$\begin{aligned} x_{k+1} &= Ax_k + Bw_k \\ y_k &= Cx_k + v_k \end{aligned} \tag{52}$$

where  $A = \begin{bmatrix} 1 & T \\ 0 & 1 \end{bmatrix}$ ,  $B = \begin{bmatrix} 0.5T^2 \\ T \end{bmatrix}$ ,  $w_k \sim \mathcal{N}(0, 1)$ ,  $C = [1 \ 0]$ , and  $T = 0.01$  is the sampling time. We consider the following two types of measurement noise:

$$\begin{cases} \text{Case 1: } v_k \sim 0.95\mathcal{N}(0, 0.1) + 0.05\mathcal{N}(0, 10) \\ \text{Case 2: } v_k \sim \mathcal{N}(0, R_t), \end{cases}$$

where  $R_t = [2(\sin(0.04\pi kT))^2 + 1]R$  and  $R = 0.1$  in Case 2. We then verify our Theorem 4 and Proposition 2 in Case 1 and 2, respectively.

TABLE III  
Performance comparison of different estimators in different cases.

Scenario	Estimators	RMSE of $x_1$	RMSE of $x_2$	avg. iteration number
Case 1	VBKF-fixed	0.053	0.081	4
	STKF	0.053	0.081	1.096
	KF	0.111	0.129	1.0
Case 2	VBKF	0.092	0.086	4
	STKF-AR1	0.092	0.086	2.190
	KF	0.130	0.143	1.0

In Case 1, all estimators use the same nominal covariance  $Q = BB^T$  and  $R = 0.1$ . Meanwhile, we adopt fixed prior inverse-Gamma parameters  $a = 2$  and  $b = 2$  in VBKF-fixed with iteration number  $N = 4$ . In STKF, we use  $\tau_i^2 = 1$  for  $i = 1, 2, 3$  and  $\nu_1 = \nu_2 \rightarrow \infty$  and  $\nu_3 = 4$  to counteract the measurement outliers. The maximum iteration number is set as  $m_{\text{iter}} = 4$  and the break condition  $\varepsilon = 0.01$ . The error performance of the VBKF-fixed, STKF, and KF is shown in Fig. 3. The corresponding root-mean-square errors (RMSE) are summarized in Table III. We observe that the performance of STKF and VBKF-fixed is identical whereas STKF has a smaller average iteration number, indicating that it possesses a higher computation efficiency. Both STKF and VBKF-fixed are significantly better than KF.

We further conduct simulations investigating the effects of  $\nu_3$  in STKF and the result is shown in Fig. 4. One can see that the error performance of the STKF first decays with the increment of  $\nu_3$  and then increases slowly, and finally coincides with the KF (We do not explicitly visualize coincidence effect to focus on the decaying-increasing trend.). In robust filtering scenarios, a too small  $\nu_i$  may induce instability (see Theorems 2) and a too large  $\nu_i$  would damage the robustify effect (see (18)). Empirically, we recommend applying  $\nu_i \in [0.1, 5]$  if the nominal noise covariances are accurate.

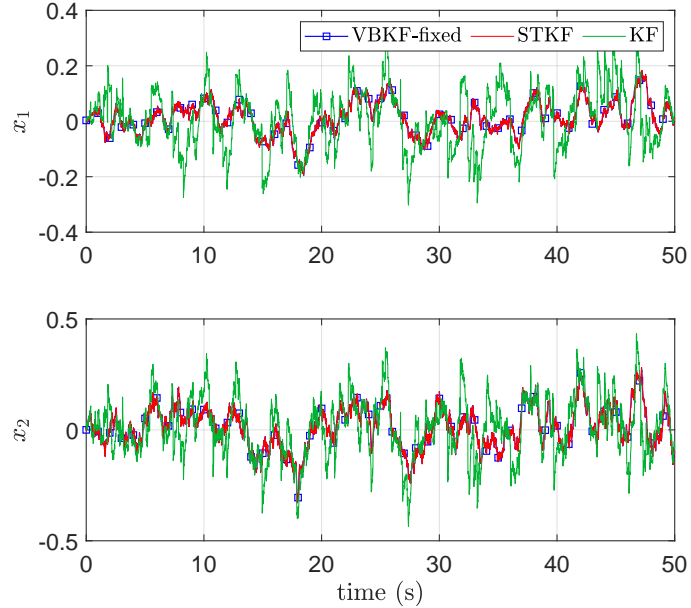


Fig. 3. Error performances of VBKF-fixed, STKF, and KF.

In Case 2 with adaptive measurement noise, we set the initial process and measurement covariance as  $Q = BB^T$ ,  $R = 0.1$ , and use  $\rho = 0.99$  in VBKF. As in STKF-AR1, we apply the same initial process and measurement covariance as is used in VBKF. Moreover, we set  $\rho_1 = \rho_2 = 1$ ,  $\rho_3 = 0.99$ ,  $\tau_i^2 = 1$  for  $i = 1, 2, 3$ ,  $\nu_1 = \nu_2 = 10^8$ , and  $\nu_3 = 100$ . The estimated covariance obtained by STKF-AR1 and by VBKF, as well as the ground measurement covariance, are visualized in Fig. 5. The corresponding error performance is summarized in Table III. We find that the performance of STKF-AR1 is identical to VBKF, but with a smaller average iteration number, which verifies Proposition 1. Both STKF-AR1 and VBKF are significantly better than KF.

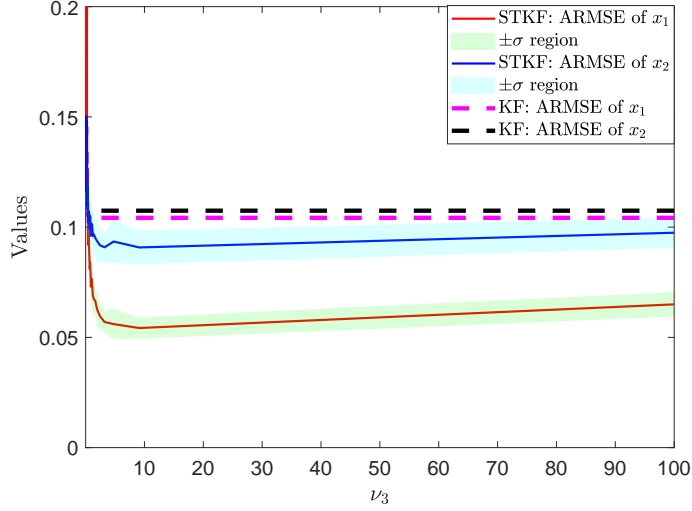


Fig. 4. Average RMSE (ARMSE) with different  $\nu_3$  in STKF.

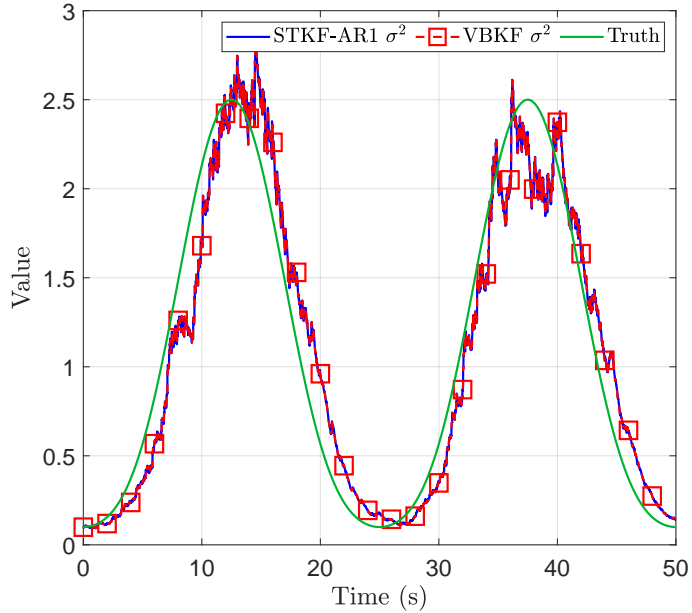


Fig. 5. The measurement noise covariance (or variance) tracking performance of VBKF and STKF-AR1.

### B. Example 2: Convergence Speed Investigation

Following system dynamics (52), we keep  $\rho_1 = \rho_2 = 1$  and investigate the effect of  $\rho_3 = \rho$  by considering the following step-like measurement covariance:

$$v_k \sim \begin{cases} \mathcal{N}(0, 0.1), & k \leq 2000 \\ \mathcal{N}(0, 2.5), & 2000 < k \leq 4000 \\ \mathcal{N}(0, 0.1), & k \geq 4000. \end{cases} \quad (53)$$

In the simulation, we compare the convergence speed of  $\rho = 0.995$ ,  $\rho = 0.99$ ,  $\rho = 0.98$ ,  $\rho = 0.97$  in Fig. 6, where the blue line denotes the ground truth variance, and the dashed black line is obtained by Theorems 5 and 6. We observe that practical convergence speed fits with the theoretical analysis very well, which verified our theorems. We plot the theoretical time constant and  $\text{Var}(\lambda_k^+)$  by assuming  $\Sigma_k = 1$  (see Theorem 5) in Fig. 7(a), and the error performance of  $x_1$  and  $x_2$  with different  $\rho$  in Fig. 7(b). The results highlight a trade-off between the convergence speed and the steady state variance.

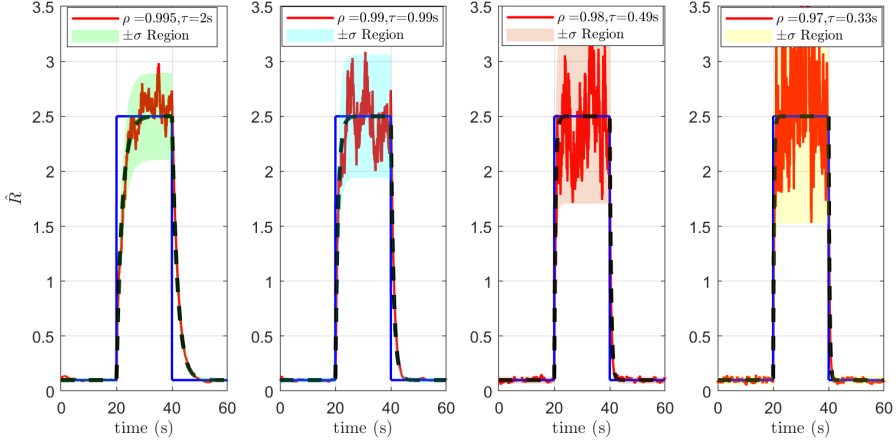


Fig. 6. Theoretical (based on Theorem 5) and practical variance convergence rate and the corresponding estimation variance with different  $\rho$ . The time constant is obtained by Theorem 6, expressed in seconds.

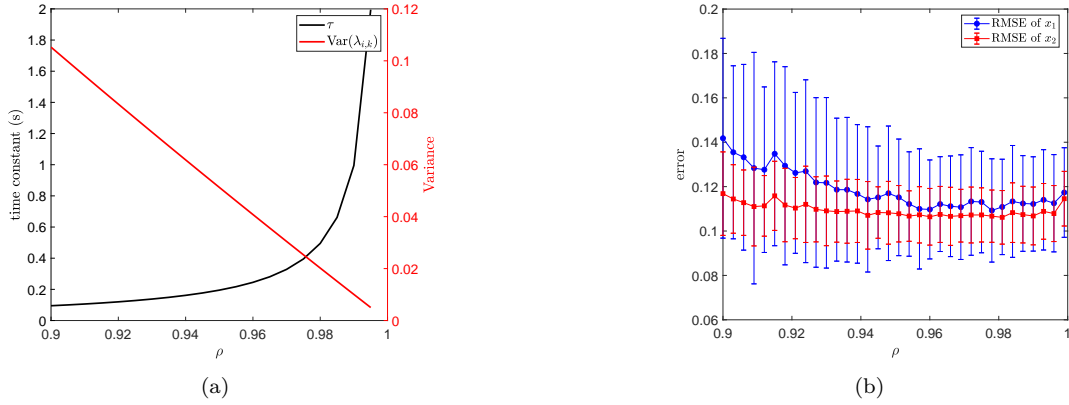


Fig. 7. The trade-off effects of  $\rho$  in STKF-AR1. (a) The trade-off between convergence time constant and convergence variance regarding  $\rho$ . (b) The error performance with different  $\rho$ .

### C. Example 4: Superior Performance

We consider a 1-DOF torsion load system with unknown disturbances as given in [38], [39]. The discrete system dynamics, with sampling time of  $dt = 0.01$  and maximum time step  $N_t = 2000$ , are given by

$$\begin{aligned} x_k &= F_k x_{k-1} + G_{1,k} u_{k-1} + G_{2,k} d_{k-1} + w_k \\ y_k &= H_k x_k + v_k \end{aligned} \quad (54)$$

with

$$\begin{aligned} F_k &= \begin{bmatrix} 0.9205 & 0.0795 & 0.0085 & 0.0003 \\ 0.2045 & 0.7955 & 0.0007 & 0.0085 \\ -14.3468 & 14.3468 & 0.6872 & 0.0746 \\ 37.5370 & -37.5370 & 0.1863 & 0.6405 \end{bmatrix} \\ G_{1,k} &= [0.0826, 0.0031, 15.5568, 1.2100]^T \\ G_{2,k} &= [0.0031, 0.2076, 1.2100, 38.7470]^T \\ H_k &= \begin{bmatrix} 1 & 0 & 0 & 0 \\ 0 & 1 & 0 & 0 \end{bmatrix}. \end{aligned}$$

where  $x_k = [\theta_m, \dot{\theta}_m, v_m, \dot{v}_m]^T \in \mathbb{R}^4$  represents the state vector, consisting of the angles at both the motor and load sides, as well as the velocities at the motor and load sides,  $u_k \in \mathbb{R}$  is the motor torque,  $d_k \in \mathbb{R}$  is the unknown disturbance,  $y_k$  is the noisy angle measurements at both motor and load sides. We augment the disturbance and the state as a new state and use a random walk model for the unknown disturbance dynamics by analogy to [6] to simultaneously

TABLE IV  
Performance comparison of different estimators in complex noise scenarios.

Scenario	Estimators	Hyper-parameters	RMSE of $x_1$	RMSE of $x_2$	RMSE of $x_3$	RMSE of $x_4$	RMSE of $x_5$
Case 1	VBKF	$\rho = 0.98$	0.710	2.609	2.717	71.101	111.818
	STKF-AR1	$\nu_p = 100 \cdot \mathbf{1}_5, \nu_r = 10^8 \mathbf{1}_2$ $\rho_p = 0.98 \cdot \mathbf{1}_5, \rho_r = \mathbf{1}_2$	0.507	0.237	0.249	58.162	64.819
	KF	$\emptyset$	0.604	0.589	0.477	55.350	71.400
	RBKF1	$\nu_p = 2 \cdot \mathbf{1}_5, \nu_r = 10^8 \cdot \mathbf{1}_2$	0.557	0.258	0.265	55.888	62.650
	RBKF2	$\nu_p = 0.5 \cdot \mathbf{1}_5, \nu_r = 1.999 \cdot \mathbf{1}_2$	0.535	0.254	0.259	55.664	60.958
	RBKF3	$\nu_p = 1 \cdot \mathbf{1}_5, \nu_r = 10^8 \cdot \mathbf{1}_2$	0.555	0.273	0.271	55.093	60.377
Case 2	VBKF	$\rho = 0.98$	0.408	0.625	0.863	32.089	58.726
	STKF-AR1	$\nu_p = 3 \cdot \mathbf{1}_5, \nu_r = 100 \mathbf{1}_2$ $\rho_p = 1 \cdot \mathbf{1}_5, \rho_r = 0.98 \cdot \mathbf{1}_2$	0.375	0.423	0.503	28.231	47.228
	KF	$\emptyset$	0.468	0.416	0.515	28.315	49.509
	RBKF1	$\nu_p = 2 \cdot \mathbf{1}_5, \nu_r = 2 \cdot \mathbf{1}_2$	0.392	2.151	2.263	35.268	62.601
	RBKF2	$\nu_p = 0.5 \cdot \mathbf{1}_5, \nu_r = 0.5 \cdot \mathbf{1}_2$	0.380	0.743	0.978	32.881	59.835
	RBKF3	$\nu_p = \mathbf{1}_5, \nu_r = \mathbf{1}_2$	0.386	0.502	0.754	30.510	56.959
Case 3	VBKF	$\rho = 0.98$	0.200	0.359	0.406	15.085	23.448
	STKF-AR2	$\nu_p = 100^8 \cdot \mathbf{1}_5, \nu_r = 100 \mathbf{1}_2$ $\rho_p = \mathbf{1}_5, \rho_r = 0.98 \cdot \mathbf{1}_2$	0.203	0.322	0.389	15.165	22.948
	KF	$\emptyset$	0.359	0.600	0.524	21.320	34.781
	RBKF1	$\nu_p = 10^8 \cdot \mathbf{1}_5, \nu_r = 2 \cdot \mathbf{1}_2$	0.229	0.428	0.508	16.257	24.640
	RBKF2	$\nu_p = 1.999 \cdot \mathbf{1}_5, \nu_r = 0.5 \cdot \mathbf{1}_2$	0.210	0.363	0.425	15.576	23.530
	RBKF3	$\nu_p = 10^8 \cdot \mathbf{1}_5, \nu_r = \mathbf{1}_2$	0.215	0.341	0.411	15.554	23.630

estimate the disturbance and state, which gives

$$\begin{aligned} \mathbf{x}_k &= \mathbf{A}_k \mathbf{x}_{k-1} + \mathbf{B}_k \mathbf{u}_{k-1} + \mathbf{w}_k \\ \mathbf{y}_k &= \mathbf{C}_k \mathbf{x}_k + \mathbf{v}_k \end{aligned} \quad (55)$$

where

$$\begin{aligned} \mathbf{x}_k &= \begin{bmatrix} d_k \\ x_k \end{bmatrix}, \quad \mathbf{w}_k = \begin{bmatrix} w_{d,k} \\ w_{x,k} \end{bmatrix}, \quad \mathbf{A}_k = \begin{bmatrix} 1 & 0_{1 \times 3} \\ G_{2,k} & F_k \end{bmatrix}, \\ \mathbf{B}_k &= \begin{bmatrix} 0 \\ G_{1,k} \end{bmatrix}, \quad \mathbf{C}_k = [0_{2 \times 1} \quad H_k], \quad \mathbf{y}_k = y_k. \end{aligned}$$

In the simulation, we consider the following three complex noise scenarios: (1) the process noise covariance is step-like where as the measurement covariance keeps constant; (2) the process noise is contaminated by outliers, where as the measurement noise covariance changes continually; (3) the process noise covariance keep constant, whereas the measurement noise covariance changes continually and is occasionally polluted by outliers.

$$\begin{aligned} \text{Case 1} &\left\{ \begin{array}{l} \mathbf{w}_k \sim \mathcal{N}(0, Q), 800 \leq k < 1200 \\ \mathbf{w}_k \sim \mathcal{N}(0, 100Q), \text{otherwise} \\ \mathbf{v}_k \sim \mathcal{N}(0, R), \end{array} \right. \\ \text{Case 2} &\left\{ \begin{array}{l} \mathbf{w}_k \sim 0.99\mathcal{N}(0, Q) + 0.01\mathcal{N}(0, 900Q) \\ \mathbf{v}_k \sim \mathcal{N}(0, R_t) \end{array} \right. \\ \text{Case 3} &\left\{ \begin{array}{l} \mathbf{w}_k \sim \mathcal{N}(0, Q) \\ \mathbf{v}_k \sim 0.99\mathcal{N}(0, R_t) + 0.01\mathcal{N}(0, 900R) \end{array} \right. \end{aligned} \quad (56)$$

where

$$\begin{aligned} Q &= \begin{bmatrix} 0.01 & 0 \\ 0 & 0.01\mathbf{I}_4 \end{bmatrix}, R = 0.5\mathbf{I}_2, \\ R_t &= [2(\sin(0.04\pi kT))^2 + 1]R \end{aligned} \quad (57)$$

We compare the performance of VBKF, STKF-AR1 (or STKF-AR2), KF-DOB, as well as RBKF1, RBKF2, and RBKF3 (by analogously applying Lines 2, 3, and 4 of Table I in Algorithm 1). Specifically, in all estimators, we apply the same nominal process covariance using  $Q^* = Q$  and  $R^* = R$ , where  $Q$  and  $R$  are shown in (57). The hyper-parameters of different estimators are tuned based on the properties of their losses and the characteristics of the noise, and are summarized in Table I. We find that our proposed methods are the best among the all filters.

We further visualize the measurement covariance tracking of VBKF and STKF-AR1 (or STKF-AR2) in Case 2 and Case 3 in Figs. 8 and 9, respectively. We find that in both cases, the conventional VBKF fails to track the ground truth noise covariance, where the tracking process is destroyed by the process outliers in Case 2 and the measurement

outliers in Case 3. Our proposed STKF-AR1 and STKF-AR2 mitigate these problems, since the proposed methods address both the outliers and adaptive noise in a unified framework.

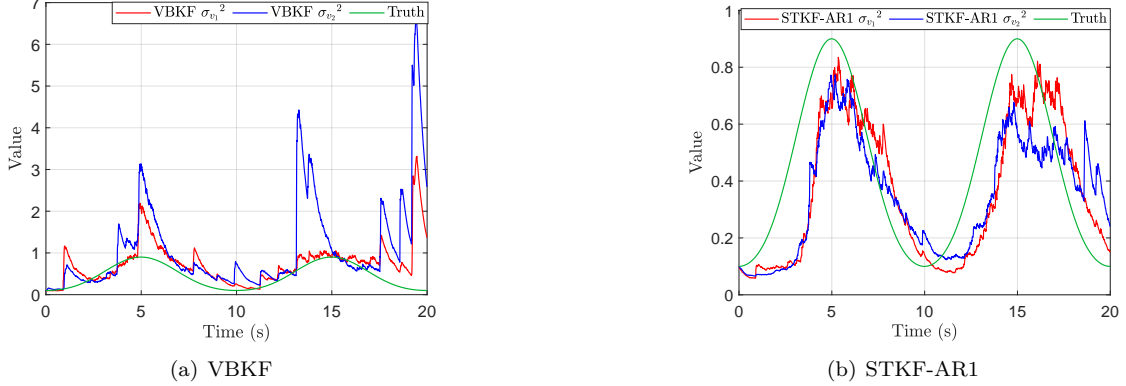


Fig. 8. The measurement covariance (or variance) tracking performance of VBKF and STKF-AR1 in Case 2. The blue and orange lines denote the estimated variance, and the yellow line denote the ground truth variance (for both two measurement channels). (a) The performance of VBKF. (b) The performance of STKF-AR1.

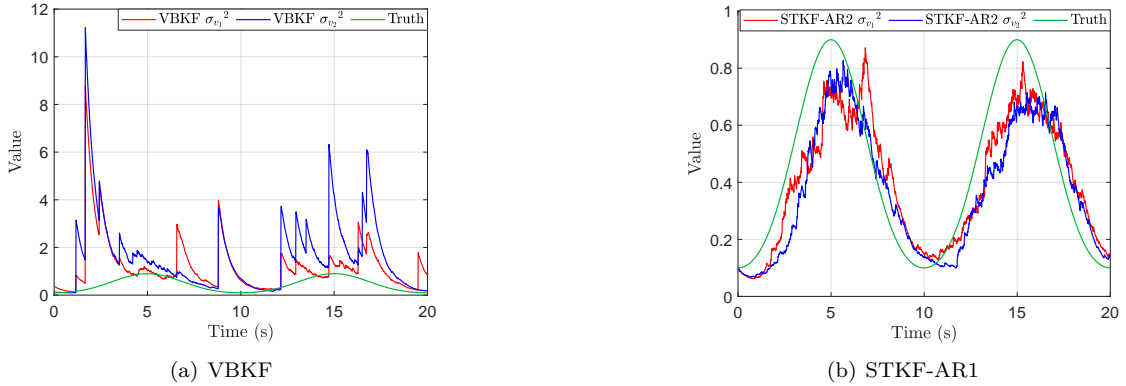


Fig. 9. The measurement covariance (or variance) tracking performance of VBKF and STKF-AR2 in Case 3. (a) The performance of VBKF. (b) The performance of STKF-AR2.

## V. Conclusion

This work bridges the gap between the robust Kalman filter and the adaptive filter. Specifically, we prove that the STKF, derived by the Student's  $t$ -distribution induced loss and solved by fixed-point iteration, can be understood as a prerequisite of the VBKF. On this basis, we provide necessary conditions for a class of losses that can be solved by a fixed-point solution, which is much more computation-efficient than gradient-based solutions. Leveraging the variational technique, we derive two robust-adaptive filters, STKF-AR1 and STKF-AR2. We demonstrate that there is a trade-off between tracking speed and tracking variance in terms of covariance tracking in adaptive filters, highlighting the importance of selecting proper forgetting factors. Our proposed approaches can recover KF, STKF (robust filters), VBKF (adaptive filters), and can address complex noise scenarios with mixing outliers and adaptive noises. Simulations verify the effectiveness of the proposed method.

## VI. Appendix

### A. Appendix A

According to Lemma 1, we know that the optimization on  $e_i$  is not related to other parts of the error ( $e_j$  with  $i \neq j$ ). Thus, one can optimize  $e_i$  for  $i = 1, 2, \dots, l$  one by one. Specifically, for  $e_i$ , we have

$$\arg \min_{e_i} \mathcal{L}_{st,i} = \frac{\nu_i + c}{2} \log \left( 1 + \frac{e_i^2}{\nu_i \tau_i^2} \right). \quad (58)$$

It is obvious that the optimization results are invariant with the scalar term. Hence, the above optimization can be equivalently written as

$$\arg \min_{e_i} \mathcal{L}_{st,i} = \frac{\nu_i}{2} \log \left( 1 + \frac{e_i^2}{\nu_i \tau_i^2} \right). \quad (59)$$

Hence, (5a) and (5b) are equivalent. This completes the proof.

## B. Appendix B

The system dynamics, according to (13), are as follow

$$t_k = W_k x_k + \zeta_k. \quad (60)$$

We follow the standard VB-approach and approximate the joint distribution using a factored form as follows

$$p(x_k, \Sigma_k | t_k) \approx Q_x(x_k) Q_\Sigma(\Sigma_k). \quad (61)$$

Then, one can minimize the Kullback-Leibler (KL) divergence between the approximated distribution and the true posterior:

$$\text{KL}(Q_x Q_\Sigma || p(x_k, \Sigma_k | t_k)) = \int Q_x Q_\Sigma \log \left( \frac{Q_x Q_\Sigma}{p(x_k, \Sigma_k | t_k)} \right) dx_k d\Sigma_k. \quad (62)$$

Minimizing KL divergence with respect to  $Q_x(x_k)$  and  $Q_\Sigma(\Sigma_k)$  gives

$$\begin{aligned} Q_x(x_k) &\propto \exp(E_{Q_\Sigma}[\log(x_k, \Sigma_k, t_k)]) \\ Q_x(\Sigma_k) &\propto \exp(E_{Q_x}[\log(x_k, \Sigma_k, t_k)]). \end{aligned} \quad (63)$$

For the first equation, it follows that

$$\begin{aligned} E_{Q_\Sigma}[\log(x_k, \Sigma_k, t_k)] &= E_{Q_\Sigma}[\log(t_k | x_k, \Sigma_k)] + E_{Q_\Sigma}[\log p(x_k)] \\ &\quad + E_{Q_\Sigma}[\log p(\Sigma_k)] \\ &= -\frac{1}{2}(t_k - W_k)^T \langle \Sigma_k^{-1} \rangle_\Sigma (t_k - W_k) \\ &\quad - \frac{1}{2}(x_k - \hat{x}_k^-)^T (P_k^-)^{-1} (x_k - \hat{x}_k^-) + C_1, \end{aligned} \quad (64)$$

where  $\langle \cdot \rangle_\Sigma = \int (\cdot) Q_\Sigma(\Sigma_k) d\Sigma_k$  denotes the expected value with respect to  $Q_\Sigma(\Sigma_k)$ ,  $\hat{x}_k^-$  denotes the prior estimate of  $x_k$ ,  $P_k^-$  is the prior covariance of  $x_k$ , and  $C_1$  is constant.

Similarly, for the second equation, one has

$$\begin{aligned} E_{Q_x}[\log(x_k, \Sigma_k, t_k)] &= E_{Q_x}[\log(t_k | x_k, \Sigma_k)] + E_{Q_x}[\log p(x_k)] \\ &\quad + E_{Q_x}[\log p(\Sigma_k)] \\ &= -\sum_{i=1}^l \left( \frac{3}{2} + \frac{\nu_{i,k}}{2} \right) \ln(\tau_{i,k}^2) - \sum_{i=1}^l \frac{\nu_{i,k}}{2} \\ &\quad - \frac{1}{2} \sum_{i=1}^l \langle (t_k - W_k x_k)_i^2 \rangle_x + C_2, \end{aligned} \quad (65)$$

where  $\langle \cdot \rangle_x = \int (\cdot) Q_x(x_k) dx_k$ . By evaluating the expectations in (64) and (65), and matching the parameters of the distributions on left and right hand sides gives

$$\begin{aligned} Q_x(x_k) &= \mathcal{N}(x_k | \hat{x}_k, P_k) \\ Q_\Sigma(\Sigma_k) &= \prod_{i=1}^l \text{Inv-Gam}(\sigma_i^2 | \frac{\nu_i}{2}, \frac{\nu_{i,k} \tau_{i,k}^2}{2}). \end{aligned} \quad (66)$$

where  $\hat{x}_k$  and  $P_k$  are obtained by the fix-point iteration by solving (16), and  $\nu_{i,k}$ ,  $\tau_{i,k}^2$  are obtained by the following equations:

$$\begin{aligned} \nu_{i,k}^+ &= \nu_{i,k}^- + 1, \\ \tau_{i,k}^2 &= (\tau_{i,k}^2)^- + \frac{e_{i,k}^T e_{i,k}}{\nu_{i,k}^+} + \frac{[W_k P_k W_k]_{ii}}{\nu_{i,k}^+}, \end{aligned} \quad (67)$$

where  $e_{i,k}$  is the  $i$ -th element of  $e_k = T_k - W_k x_k$ . This completes the proof.

### C. Appendix C

Proof 11: It is obvious that STKF-AR1 is identical to STKF when  $\rho_i = 1$  for all  $i = 1, 2, \dots, l$ . We then focus on the second part of the proof. According to (14), the unified objective function has

$$\begin{aligned} J(x_k, \nu_{i,k}, \nu_{j,k}, \tau_{i,k}^2, \tau_{j,k}^2) &= \sum_{i=1}^n \frac{\nu_i}{2} \log \left( 1 + (e_{i,k}^T e_{i,k}) / (\nu_i * \tau_i^2) \right) \\ &+ \sum_{j=n+1}^{n+m} \frac{\nu_j}{2} \log \left( 1 + (e_{j,k}^T e_{j,k}) / (\nu_j * \tau_j^2) \right), \end{aligned} \quad (68)$$

where  $e_{i,k}$  is an element of normalized process error  $e_{p,k} = [e_{1,k}, \dots, e_{1,k}] = (P_k^-)^{-1/2}(x_k - \hat{x}_k^-)$ ,  $e_{j,k}$  is an element of normalized measurement error  $e_{r,k} = [e_{n+1,k}, \dots, e_{n+m,k}] = (R_k)^{-1/2}(y_k - Cx_k)$  with  $j \in [n+1, n+m]$ . In situations that  $\rho_i = 1$ ,  $\nu_i \rightarrow \infty$ , and  $\rho_j = \rho_c$ , according to Property 1, we have

$$\begin{aligned} J(x_k, \nu_{j,k}, \tau_{j,k}^2) &= \frac{1}{2}(x_k - \hat{x}_k^-)^T (P_k^-)^{-1}(x_k - \hat{x}_k^-) \\ &+ \sum_{j=n+1}^{n+m} \frac{\nu_j}{2} \log \left( 1 + (e_{j,k}^T e_{j,k}) / (\nu_j * \tau_j^2) \right). \end{aligned} \quad (69)$$

According to Theorem 4 and the exponentiation mapping between the objective function and the probability density function, the loss (69) corresponds to the following MAP problem:

$$\begin{aligned} p(x_k, R_{v_k v_k^T} | y_k) &\propto p(x_k | y_{1:k-1}) p(x_k, R_{v_k v_k^T} | y_k) \\ &= p(x_k | y_{1:k-1}) p(x_k | R_{v_k v_k^T}, y_k) p(R_{v_k v_k^T}) \end{aligned} \quad (70)$$

with

$$\begin{aligned} p(x_k | y_{1:k-1}) &= \frac{\exp \left( - (x_k - A\hat{x}_{k-1})^T (P_k^-)^{-1}(x_k - A\hat{x}_{k-1}) \right)}{\sqrt{(2\pi)^n |P_k^-|}} \\ p(x_k, R_{v_k v_k^T} | y_k) &= \frac{\exp \left( - (y_k - Cx_k)^T R_k^{-1} R_{v_k v_k^T}^{-1} (y_k - Cx_k) \right)}{\sqrt{(2\pi)^m |R_k R_{v_k v_k^T}|}} \\ p(R_{v_k v_k^T}) &= \prod_{j=n+1}^l \frac{(\nu_j \tau_j^2 / 2)^{\nu_j/2}}{\Gamma(\nu_j/2)} \lambda_j^{-(\nu_j/2+1)} \exp \left( - \frac{\nu_j \tau_j^2}{2\lambda_j} \right) \\ R_{v_k v_k^T} &= \text{diag}[\lambda_{n+1}, \lambda_{n+2}, \dots, \lambda_l]. \end{aligned} \quad (71)$$

We observe that the objective function is identical to [24], which completes the proof.

### D. Appendix D

Laplace approximation uses a second-order Taylor expansion of  $\ln p(\lambda)$  at  $\lambda = \lambda_0$  [see  $p(\lambda)$  in (3)]:

$$\begin{aligned} \ln p(\lambda) &\approx \ln p(\lambda_0) + \underbrace{\frac{d}{d\lambda} \ln p(\lambda) \Big|_{\lambda_0}}_a (\lambda - \lambda_0) \\ &+ \underbrace{\frac{1}{2} \frac{d^2}{d\lambda^2} \ln p(\lambda) \Big|_{\lambda_0}}_b (\lambda - \lambda_0)^2. \end{aligned} \quad (72)$$

Denote  $\lambda_0 = \frac{\nu\tau^2}{\nu+1}$ , it follows that

$$\begin{aligned} \ln p(\lambda) &\approx \ln p(\lambda_0) + \frac{1}{2\tau^2} \left( \lambda - \frac{\nu\tau^2}{\nu+1} \right) \\ &- \frac{1}{2} \frac{(\nu+1)^3}{2\nu^2\tau^4} \left( \lambda - \frac{\nu\tau^2}{\nu+1} \right)^2. \end{aligned} \quad (73)$$

In Gaussian distribution, one has

$$\ln q(\lambda; \mu, \sigma^2) = -\frac{\lambda^2}{2\sigma^2} + \frac{\lambda\mu}{\sigma^2} - \frac{\mu^2}{2\sigma^2}.$$

By matching the terms, one has

$$q(\lambda; \mu, \sigma^2) \sim \mathcal{N}(\tau^2, \frac{2\nu^2\tau^4}{(\nu+1)^3}).$$

## References

- [1] T. D. Barfoot, J. R. Forbes, and D. J. Yoon, "Exactly sparse Gaussian variational inference with application to derivative-free batch nonlinear state estimation," *The International Journal of Robotics Research*, vol. 39, no. 13, pp. 1473–1502, 2020.
- [2] A. Harvey, E. Ruiz, and N. Shephard, "Multivariate stochastic variance models," *The Review of Economic Studies*, vol. 61, no. 2, pp. 247–264, 1994.
- [3] A. Keil, "Dynamic variational level sets for cardiac 4d reconstruction," Ph.D. dissertation, Technische Universität München, 2010.
- [4] P. L. Houtekamer and F. Zhang, "Review of the ensemble Kalman filter for atmospheric data assimilation," *Monthly Weather Review*, vol. 144, no. 12, pp. 4489–4532, 2016.
- [5] K. Course and P. B. Nair, "State estimation of a physical system with unknown governing equations," *Nature*, vol. 622, no. 7982, pp. 261–267, 2023.
- [6] S. Li, D. Shi, Y. Lou, W. Zou, and L. Shi, "Generalized multi-kernel maximum correntropy Kalman filter for disturbance estimation," *IEEE Transactions on Automatic Control*, 2023.
- [7] T. Nishimura, "On the a priori information in sequential estimation problems," *IEEE Transactions on Automatic Control*, vol. 11, no. 2, pp. 197–204, 1966.
- [8] M. Grimble, " $H_\infty$  design of optimal linear filters," *Linear Circuit Systems and Signal Processing: Theory and Application (Proc. MTNS'87)*, pp. 533–540, 1988.
- [9] L. Chang, B. Hu, G. Chang, and A. Li, "Huber-based novel robust unscented Kalman filter," *IET Science, Measurement & Technology*, vol. 6, no. 6, pp. 502–509, 2012.
- [10] A. K. Roonizi, " $\ell_2$  and  $\ell_1$  trend filtering: A Kalman filter approach," *IEEE Signal Processing Magazine*, vol. 38, no. 6, pp. 137–145, 2021.
- [11] G. Wang, C. Yang, and X. Ma, "A novel robust nonlinear Kalman filter based on multivariate Laplace distribution," *IEEE Transactions on Circuits and Systems II: Express Briefs*, vol. 68, no. 7, pp. 2705–2709, 2021.
- [12] Y. Huang, Y. Zhang, N. Li, Z. Wu, and J. A. Chambers, "A novel robust student's t-based Kalman filter," *IEEE Transactions on Aerospace and Electronic Systems*, vol. 53, no. 3, pp. 1545–1554, 2017.
- [13] J. C. Principe, *Information theoretic learning: Renyi's entropy and kernel perspectives*. Springer Science & Business Media, 2010.
- [14] V. Vapnik, *The nature of statistical learning theory*. Springer science & business media, 2013.
- [15] S. Li, D. Shi, W. Zou, and L. Shi, "Multi-kernel maximum correntropy Kalman filter," *IEEE Control Systems Letters*, vol. 6, pp. 1490–1495, 2021.
- [16] B. Chen, X. Liu, H. Zhao, and J. C. Principe, "Maximum correntropy Kalman filter," *Automatica*, vol. 76, pp. 70–77, 2017.
- [17] S. Li, D. Shi, Y. Lou, W. Zou, and L. Shi, "Generalized multi-kernel maximum correntropy Kalman filter for disturbance estimation," *IEEE Transactions on Automatic Control*, 2023.
- [18] M. Bai, Y. Huang, Y. Zhang, and J. Chambers, "Statistical similarity measure-based adaptive outlier-robust state estimator with applications," *IEEE Transactions on Automatic Control*, vol. 67, no. 8, pp. 4354–4361, 2022.
- [19] M. V. Kulikova, "Chandrasekhar-based maximum correntropy Kalman filtering with the adaptive kernel size selection," *IEEE Transactions on Automatic Control*, vol. 65, no. 2, pp. 741–748, 2019.
- [20] A. Singh and J. C. Principe, "Using correntropy as a cost function in linear adaptive filters," in *2009 International Joint Conference on Neural Networks*. IEEE, 2009, pp. 2950–2955.
- [21] B. Chen, J. Wang, H. Zhao, N. Zheng, and J. C. Principe, "Convergence of a fixed-point algorithm under maximum correntropy criterion," *IEEE Signal Processing Letters*, vol. 22, no. 10, pp. 1723–1727, 2015.
- [22] R. Kashyap, "Maximum likelihood identification of stochastic linear systems," *IEEE Transactions on Automatic Control*, vol. 15, no. 1, pp. 25–34, 1970.
- [23] Y. Meng, S. Gao, Y. Zhong, G. Hu, and A. Subic, "Covariance matching based adaptive unscented Kalman filter for direct filtering in ins/gnss integration," *Acta Astronautica*, vol. 120, pp. 171–181, 2016.
- [24] S. Sarkka and A. Nummenmaa, "Recursive noise adaptive Kalman filtering by variational bayesian approximations," *IEEE Transactions on Automatic control*, vol. 54, no. 3, pp. 596–600, 2009.
- [25] Y. Huang, Y. Zhang, Z. Wu, N. Li, and J. Chambers, "A novel adaptive Kalman filter with inaccurate process and measurement noise covariance matrices," *IEEE transactions on Automatic Control*, vol. 63, no. 2, pp. 594–601, 2017.
- [26] D. Ćetenović, J. Zhao, V. Levi, Y. Liu, and V. Terzija, "Variational bayesian unscented Kalman filter for active distribution system state estimation," *IEEE Transactions on Power Systems*, 2024.
- [27] P. Dong, Z. Jing, H. Leung, and K. Shen, "Variational bayesian adaptive cubature information filter based on wishart distribution," *IEEE Transactions on Automatic Control*, vol. 62, no. 11, pp. 6051–6057, 2017.
- [28] A. Aravkin, J. V. Burke, L. Ljung, A. Lozano, and G. Pillonetto, "Generalized Kalman smoothing: Modeling and algorithms," *Automatica*, vol. 86, pp. 63–86, 2017.
- [29] B. Chen, L. Xing, H. Zhao, N. Zheng, J. C. Pri et al., "Generalized correntropy for robust adaptive filtering," *IEEE Transactions on Signal Processing*, vol. 64, no. 13, pp. 3376–3387, 2016.
- [30] G. Chang, C. Chen, Q. Zhang, and S. Zhang, "Variational bayesian adaptation of process noise covariance matrix in Kalman filtering," *Journal of the Franklin Institute*, vol. 358, no. 7, pp. 3980–3993, 2021.
- [31] G. Chang, "Kalman filter with both adaptivity and robustness," *Journal of Process Control*, vol. 24, no. 3, pp. 81–87, 2014.
- [32] K. Li, L. Chang, and B. Hu, "A variational bayesian-based unscented Kalman filter with both adaptivity and robustness," *IEEE Sensors Journal*, vol. 16, no. 18, pp. 6966–6976, 2016.
- [33] A. Gelman, J. B. Carlin, H. S. Stern, and D. B. Rubin, *Bayesian data analysis*. Chapman and Hall/CRC, 1995.
- [34] M. West, "Outlier models and prior distributions in bayesian linear regression," *Journal of the Royal Statistical Society Series B: Statistical Methodology*, vol. 46, no. 3, pp. 431–439, 1984.
- [35] J. Vanhatalo, P. Jylänki, and A. Vehtari, "Gaussian process regression with student's t likelihood," *Advances in Neural Information Processing Systems*, vol. 22, 2009.
- [36] T. D. Barfoot, *State estimation for robotics*. Cambridge University Press, 2024.
- [37] B. G. Liptak, *Instrument Engineers' Handbook, Volume One: Process Measurement and Analysis*. CRC press, 2003.
- [38] S. Zhao, Y. S. Shmaliy, P. Shi, and C. K. Ahn, "Fusion Kalman/UFIR filter for state estimation with uncertain parameters and noise statistics," *IEEE Transactions on Industrial Electronics*, vol. 64, no. 4, pp. 3075–3083, 2016.
- [39] X. Luan, W. Xue, S. Zhao, and F. Liu, "A Kalman & fading memory co-filter for uncertain systems based on self-perception mechanism," *IEEE Transactions on Automatic Control*, 2025.

PLACE  
PHOTO  
HERE

Shilei Li received the B.E. degree in Detection Guidance and Control Technology and M.S. degree in Control Engineering both from Harbin Institute of Technology, Harbin, China, in 2015 and 2018 respectively, and the Ph.D. degree in Electronic and Computer Engineering from The Hong Kong University of Science and Technology, Hong Kong, China, in 2022. Currently, he is an assistant professor at the School of Automation, Beijing Institute of Technology, China. His research interests include information theoretic learning, orientation estimation of IMUs, synchronization control, human-robot interaction, and exoskeleton robots.

PLACE  
PHOTO  
HERE

Dawei Shi received the B.E. degree in Electrical Engineering and Automation from the Beijing Institute of Technology, Beijing, China, in 2008, the Ph.D. degree in Control Systems from the University of Alberta, Edmonton, AB, Canada, in 2014. In December 2014, he was appointed as an Associate Professor at the School of Automation, Beijing Institute of Technology. From February 2017 to July 2018, he was with the Harvard John A. Paulson School of Engineering and Applied Sciences, Harvard University, as a Postdoctoral Fellow in bioengineering. Since July 2018, he has been with the School of Automation, Beijing Institute of Technology, where he is a professor. His research focuses on the analysis and synthesis of complex sampled-data control systems with applications to biomedical engineering, robotics, and motion systems. He serves as an Associate Editor/Technical Editor for IEEE Transactions on Industrial Electronics, IEEE/ASME Transactions on Mechatronics, IEEE Control Systems Letters, and IET Control Theory and Applications. He is a member of the Early Career Advisory Board of Control Engineering Practice. He was a Guest Editor for European Journal of Control. He served as an associate editor for IFAC World Congress and is a member of the IEEE Control Systems Society Conference Editorial Board. He is a Senior Member of the IEEE.

PLACE  
PHOTO  
HERE

Hao Yu received the BS and the PhD degrees in Control Theory and Engineering from Beihang University, China, in 2013 and 2018, respectively. From 2019 to 2022, he was a Postdoctoral Fellow in the Department of Electrical and Computer Engineering, at the University of Alberta, Canada. He is presently a Professor in the School of Automation at Beijing Institute of Technology, China. His research interests include hybrid systems, event-triggered control, multi-agent systems, data-driven PID control, adaptive control and cyber-physical systems.

PLACE  
PHOTO  
HERE

Ling Shi received his B.E. degree in Electrical and Electronic Engineering from The Hong Kong University of Science and Technology (HKUST) in 2002 and Ph.D. degree in Control and Dynamical Systems from The California Institute of Technology (Caltech) in 2008. He is currently a Professor in the Department of Electronic and Computer Engineering at HKUST with a joint appointment in the Department of Chemical and Biological Engineering (2025-2028). His research interests include cyber-physical systems security, networked control systems, sensor scheduling, event-based state estimation, and multi-agent robotic systems (UAVs and UGVs). He served as an editorial board member for the European Control Conference 2013-2016. He was a subject editor for International Journal of Robust and Nonlinear Control (2015-2017), an associate editor for IEEE Transactions on Control of Network Systems (2016-2020), an associate editor for IEEE Control Systems Letters (2017-2020), and an associate editor for a special issue on Secure Control of Cyber Physical Systems in IEEE Transactions on Control of Network Systems (2015-2017). He also served as the General Chair of the 23rd International Symposium on Mathematical Theory of Networks and Systems (MTNS 2018). He is currently serving as a member of the Engineering Panel (Joint Research Schemes) of the Hong Kong Research Grants Council (RGC) (2023-2026). He received the 2024 Chen Han-Fu Award given by the Technical Committee on Control Theory, Chinese Association of Automation (TCCT, CAA). He is a member of the Young Scientists Class 2020 of the World Economic Forum (WEF), a member of The Hong Kong Young Academy of Sciences (YASHK), and he is an IEEE Fellow.